Descriptive Analysis of a Virtual Transect through the Benguela Upwelling System

By

Nicolette Chang

Submitted in partial fulfilment of the requirements for the degree
Master of Science
in the Faculty of Science at the UNIVERSITY OF CAPE TOWN

March 2003

Supervisors:
Assoc. Prof. F.A. Shillington (Dept. of Oceanography)
Dr. C. Roy (Institut de Recherche pour le Developpement
Research Associate at the Dept. of Oceanography)

ABSTRACT

With the limitations of *in situ* observations of the ocean, numerical modeling of the ocean can easily provide clues to the structures and processes that lie therein. This project is an example of the examination of numerical model output. In this case, the area of interest is an area of ocean off Namaqualand which displays a reaction to local wind forcing. A transect was performed off the coast using output from ROMS (Regional Ocean Modeling System), forced under realistic winds obtained from weekly averaged ERS data. Temporal and spatial analysis yield information on the climatological characteristics of this region. Subsurface poleward flow was observed at the shelf break, and reached a maximum speed of 5 $cm.s^{-1}$ in March. In addition, it was observed that the subsurface poleward flow was not apparent when equatorward surface flow was maximum in intensity and spatial extent.

CONTENTS

ABSTRACT 2

CONTENTS 3

List of Figures 4

INTRODUCTION 6

CHAPTER 1 – Benguela Current System
- 1.1 Geographical setting 8
- 1.2 Circulation and Water Masses 10
- 1.3 Atmospheric forcing 13
- 1.4 Features of the Benguela 16
- 1.5 Shelf and Shelf-break circulation 19
- 1.6 Benguela Variability 21
- 1.7 General Hydrographic features of the shelf and slope 26

CHAPTER 2 – Modeling the Coastal Ocean
- 2.1 Previous models of the Benguela 25
- 2.2 Description of ROMS 26
- 2.3 Limitations of ROMS 29
- 2.4 Model Applications 29

CHAPTER 3 – Methodology
- 3.1 Data 30
- 3.2 Data processing 32

CHAPTER 4 - Results 33

CHAPTER 5 – Discussion 67

CHAPTER 6 – Concluding Remarks 71

REFERENCE LIST 72

ACKNOWLEDGEMENTS 73

List of Figures

Figure 1.1	Geographical features of the Benguela Upwelling Area (Nelson & Hutchings, 1983).
Figure 1.2	Circulation in the southern Atlantic Ocean (Adapted from Tomczak, 1996).
Figure 1.3	Principal water masses comprising of the Benguela Upwelling System (Shannon and Nelson, 1996).
Figure 1.4(1-e)	Cyclic weather conditions over the Benguela (typical of summer).
Figure 1.5	Schematic flow field of surface and thermocline waters (Adapted from Stramma & Peterson, 1989 in Shannon & Nelson, 1996).
Figure 1.6	Percentage of wind contribution. Shaded areas indicate areas of significant contribution by winds (Blanke *et al.*, 2002).
Figure 2.1	The ROMS spatial grid (left) (Penven *et al.*, 2001) and the vertical grid (right) over the southern Benguela.
Figure 3.1	Horizontal grid showing the transect in blue and the position of the four moorings (red triangles).
Figure 3.2	Vertical grid of the transect, with the four moorings shown in blue.
Figure 4.1 (a-f)	Vertical section of temperature (°C) monthly climatology (January – June). Inset: Zoom of upper 300m of section.
Figure 4.1 (g-l)	Vertical section of temperature (°C) monthly climatology (July – December). Inset: Zoom of upper 300m of section.
Figure 4.2(a-f)	Vertical section of smoothed temperature standard deviation (°C) monthly climatology (January - June). Inset: Zoom of upper 300m of section.
Figure 4.2(a-f)	Vertical section of smoothed temperature standard deviation (°C) monthly climatology (January - June). Inset: Zoom of upper 300m of section.
Figure 4.2(g-l)	Vertical section of smoothed temperature (°C) standard deviation monthly climatology (July – December). Inset: Zoom of upper 300m of section.
Figure 4.3 (a - f)	Vertical section of the monthly climatology of cross-shore current ($cm.s^{-1}$) for the transect (January – June). Solid line = offshore flow, dashed line = onshore flow. Inset: Zoom of upper 300m of section.
Figure 4.3 (g-l)	Vertical section of the monthly climatology of cross-shore current ($cm.s^{-1}$) for the transect (July – December). Solid line = offshore flow, dashed line = onshore flow. Inset: Zoom of upper 300m of section.
Figure 4.4 (a-f)	Vertical section of the standard deviation of cross-shore current ($cm.s^{-1}$) for the transect (January – June). Inset: Zoom of upper 300m of section.

Figure 4.4 (g-l)	Vertical section of the standard deviation of cross-shore current ($cm.s^{-1}$) for the transect (July – December). Inset: Zoom of upper 300m of section.
Figure 4.5 (a - f)	Vertical section of the monthly climatology of alongshore current ($cm.s^{-1}$) for the transect (January – June). Solid line = equatorward flow, dashed line = poleward flow. Red line = O $cm.s^{-1}$ isotach. Inset: Zoom of upper 300m of section.
Figure 4.5 (g - l)	Vertical section of the monthly climatology of alongshore current ($cm.s^{-1}$) for the transect (July – December). Solid line = equatorward flow, dashed line = poleward flow. Red line = O $cm.s^{-1}$ isotach. Inset: Zoom of upper 300m of section.
Figure 4.6 (a - f)	Vertical section of the standard deviation of alongshore current ($cm.s^{-1}$) for the transect (January – June). Inset: Zoom of upper 300m of section.
Figure 4.6 (g - l)	Vertical section of the standard deviation of alongshore current ($cm.s^{-1}$) for the transect (July – December). Inset: Zoom of upper 300m of section.
Figure 4.7	Hovmöller plot over the transect of (a) Temperature (°C) (b) Cross-shore current ($cm.s^{-1}$) (c) Alongshore current ($cm.s^{-1}$).
Figure 4.8	Hovmöller plot over the transect of standard deviation for: (a) Temperature (°C) (b) Cross-shore current ($cm.s^{-1}$) (c) Alongshore current ($cm.s^{-1}$).
Figure 4.9	Climatological time series with depth for Mooring A of: (a) temperature(°C) (b) cross-shore current ($cm.\ s^{-1}$) (c) alongshore current ($cm.\ s^{-1}$).
Figure 4.10	Climatological time series with depth for Mooring B of: (a) temperature(°C) (b) cross-shore current ($cm.\ s^{-1}$) (c)alongshore current ($cm.\ s^{-1}$).
Figure 4.11	Climatological time series with depth for Mooring C of: (a) temperature (°C) (b) cross-shore current ($cm.\ s^{-1}$) (c) longshore current ($cm.\ s^{-1}$).
Figure 4.12	Climatological time series with depth for Mooring D of: (a) temperature (°C) (b) cross-shore current ($cm.\ s^{-1}$) (c) longshore current ($cm.\ s^{-1}$).
Figure 4.13	Depth of isotherms (metres) over the mid-shelf at Mooring B. Dashed lines = standard deviation.
Figure 4.14	Depth of isotherms (metres) over the shelf break at Mooring C. Dashed lines = standard deviation.

INTRODUCTION

Wind-driven upwelling is a feature associated with many of the world's productive fishing areas. One such region is the coast off southwest Africa, the Benguela Upwelling region. In addition, another industry based off the southwest African coast is the gas and oil industry. These marine industries have associated risks and are therefore reliant on the weather and oceanic conditions.

In order to adequately describe the oceanic conditions, many repeated measurements over time, covering the spatial extent of the area need to be performed. This process is both tedious and costly. The development and improvement of oceanic models combined with decreasing computer and processing costs can therefore play a role in describing and understanding the oceanic environment and processes in specific regions.

In an article by Blanke, Roy, Penven, Speich, McWilliams and Nelson (2002), using the numerical model ROMS, an independent region off the west coast of South Africa was found to respond favourably to interannual wind forcing as seen by sea surface temperature anomalies. The model simulates hydrographic processes and features that occur in the marine environment in response to meteorological (particularly wind) conditions. ROMS (Regional Ocean Modeling System) is a three-dimensional numerical model which is the latest evolution of the SPEM and SCRUM models. ROMS was used due to the little success gained by the use of the Princeton Ocean Model and its inability to adequately resolve mesoscale features in the southern Benguela (Penven, 2000).

In order to investigate the unusual area noted by Blanke *et al.* (2002), a transect offshore was chosen that incorporates this region. Using the output from the numerical model ROMS which was forced by realistic satellite-derived winds, a "virtual cruise" was undertaken in which "measurements" of temperature, cross-shore and alongshore currents were taken every two days for ten years, corresponding to July 1991 to December 2000. Using this data a climatological

analysis of the region was performed, thus giving the general characteristics of the region over an average year.

In this investigation, in order to understand the dynamics and processes that were observed, the general characteristics of the Benguela have been described. Due to the spatial extent and variability of the Benguela Upwelling Region, previous literature has been based mostly in certain regions such as off the Cape Peninsula (investigations into the coastal jet) and St Helena Bay. There are a few summaries of the region as a whole by certain authors who have done extensive research into and literature reviews of the region, these include Nelson and Hutchings (1983), Shannon and Nelson (1996) and Shillington (1998). Many references to their works have been used in this investigation

Also described is the use of numerical models in the coastal ocean. In particular, the model ROMS, which is used in this investigation, is briefly discussed along with its limitations. In-depth studies into ROMS and its relationship to the southern Benguela have been performed and have been discussed in Penven (2000) and Penven, Roy, Brundrit, Colin de Verdiere, Freon, Johnson, Lutjeharms, and Shillington (2001).

This investigation of the model data was carried out as if the observer had collected the data *in situ* off the coast in a repeated monitoring line performed every two days or by the placement of moorings. It would be difficult to sample the real ocean to obtain similar resolution to the model. Moorings would have to be equipped with current and temperature sensors in addition to other instruments at various locations along the study area, in order to obtain the temporal resolution as has been done here. "Virtual moorings" were placed at four locations along the transect and were analysed.

1. The Benguela Upwelling Region

The Benguela Current System, together with the California Current, the Peru Upwelling and the Canary Current, form the four main eastern boundary current regions of the World's oceans. Typical of these upwelling regions are highly productive commercial fisheries as well as industries concerning mineral and hydrocarbons resources.

1.1 Geographical Setting

The Benguela Upwelling System (Figure 1.1) is situated on the wide southwestern shelf of Africa and is bounded by the warm Agulhas current in the south at 34°S and the warm Angolan waters to the North at 10°N (Shillington, 1998).

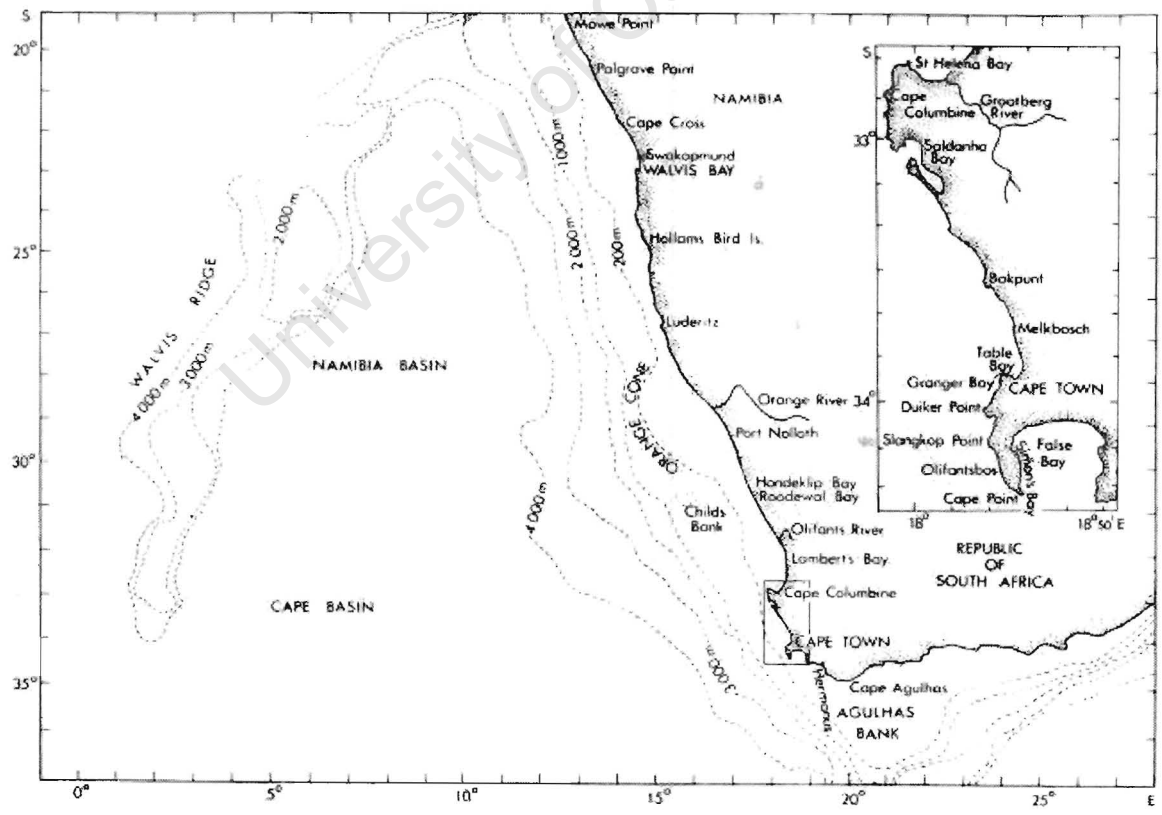

Figure 1.1: Geographical features of the Benguela Upwelling Area (Nelson & Hutchings, 1983).

The coastline between these boundaries is meridional in orientation and is fairly regular with embayments and headlands concentrated in the south, with a large peninsula south of Cape Town (Cape Peninsula). In addition, there are intrusions of several river systems into this coastline with the Orange, Cunene, Olifants and Berg Rivers being the most extensive, although the freshwater introduced by these rivers to the coast is not significant except during flooding (Shillington, 1998; Shannon & Nelson, 1996).

Comprising the bathymetry adjacent to the coast in the Benguela Upwelling Region are the Cape and Angola Basins separated by the Walvis Ridge at 18°S (Figure 1.1). The Walvis Ridge runs in a southwesterly direction from the coast to the Mid-Atlantic Ridge and forms a barrier to the flow of water below 3000m. The Cape Basin is bounded in the south by the Agulhas Ridge parallel to the Walvis Ridge and features numerous volcanic seamounts. Forming the eastern border of the basins is the continental shelf (indicated by the 200m contour) which varies from 20km wide off southern Angola and 40km off the Cape Peninsula to 180km off the Orange River. The topography of the continental shelf is relatively smooth with the shelf break at 250m. In the southern Benguela, the shelf between 32°S and 33°S varies in width. Features found in this region include an inner and outer shelf break (200-380m and 500m) between 31°S and 33°S which merge south of 33°S and several submarine canyons along the shelf (Nelson & Hutchings, 1983; Shannon & Nelson, 1996; Shillington, 1998).

1.2 Circulation and Water Masses

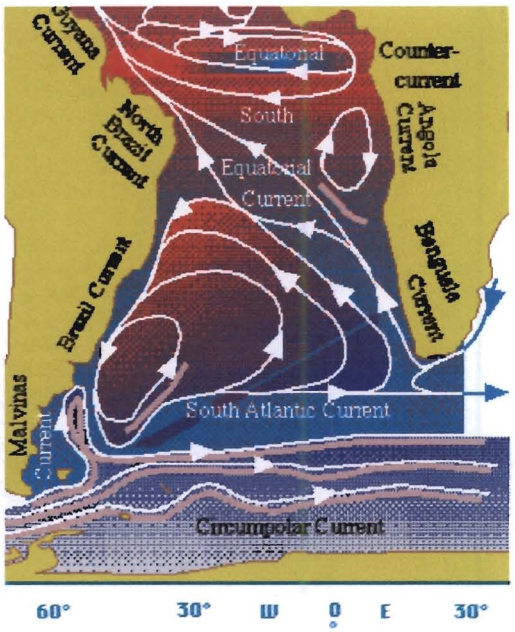

Figure 1.2: Circulation in the southern Atlantic Ocean (Adapted from Tomczak, 1996).

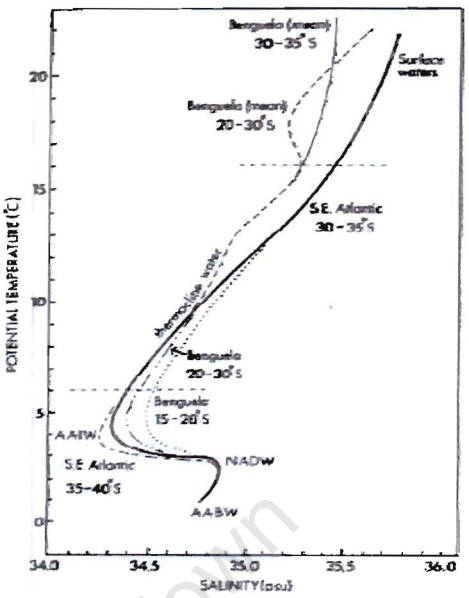

Figure 1.3: Principal water masses comprising of the Benguela Upwelling System (Shannon and Nelson, 1996).

Circulation over the South Atlantic is in the form of an anticyclonic gyre consisting of South Atlantic Central water (Sverdrup, Johnson, & Fleming, 1942 in Nelson & Hutchings, 1983) of which the Benguela Current forms the eastern limb. Gordon, Weiss, Smethie Jr. and Warner (1992, in Garzoli & Gordon, 1996) list three possible sources of water contributing to the Benguela Current (Figure 1.2):

1. the South Atlantic Current (the southern limb of the South Atlantic subtropical gyre);
2. the Agulhas Current (through the shedding of eddies from the Agulhas retroflection) made up primarily of Indian Ocean Water ; and
3. the Antarctic Circumpolar Current.

Based on results obtained during the BEST program (Benguela Sources and Transport) from June 1992 to November 1993 by Garzoli, Gordon, Kamenkovich, Pillsbury and Duncombe-Rae (1996), the water in the Benguela Current is derived from the central Atlantic – possibly primarily South Atlantic water (50%); Indian Ocean water (25%); and a mixture of Agulhas and tropical Atlantic water (25%). Water from the Indian Ocean is introduced into the Benguela Current by the eddy-shedding process occurring at the Agulhas Retroflection region, additional Indian

Ocean water may enter through the branching of the Agulhas Current at the continental shelf (Garzoli & Gordon, 1996). Subantarctic surface water may be entrained via the eddy-shedding process from the Antarctic Circumpolar Current into the Benguela Current or via the flow of the South Atlantic Current through exchanges Cross the subtropical front.

Contributing to the circulation in the southern Atlantic and to the Benguela Current are eddies of both Agulhas and Brazilian origin, these can be identified by a positive salinity anomaly and a thermostad of near 16°C and 13°C respectively (Olson, Fine & Gordon, 1992 in Garzoli & Gordon, 1996).

In the BEST program Garzoli *et al.* (1996) illustrated that the Benguela Current flow is not stationary but consists of a steady flow at the coast and a transient flow of the western part of the current (composed of large eddies), as seen at 30°S. The Benguela Current transport is very variable and the BEST data suggests that this is due to the source water, "the source of the Benguela Current may change spatially and temporally as the ratio of potential source waters changes" (Garzoli *et al.*, 1996, p. 1056). Increases in thermocline salinity were found to correspond positively with northward transport of the current indicating that the Benguela increases in strength by taking in more subtropical water.

A review of literature of the constituent water masses relevant to the Benguela is provided by Shannon and Nelson (1996). The principle water masses comprising the "core" characteristics of the Benguela Current are displayed in Figure 1.3. Important to the Benguela is thermocline water, depicted by the linear part of the θS curve (34.5-35.5 psu and 6-16°C), which is brought to the surface in upwelling and comprise the waters over the shelf, although in a much altered form. Thermocline water overlies Antarctic Intermediate Water (AAIW) at 34.2-34.5 psu and potential temperatures of 4-5°C in the Benguela, with its core at an average depth of 700-800m in the South-east Atlantic and deeper at (1100m) in the South Indian Ocean and Agulhas Retroflection area. AAIW of various origins is found in the Benguela, differing both in salinity and oxygenation, these origins include: the Indian Ocean, the South Atlantic Current and the tropical Atlantic.

North Atlantic Deep Water (NADW) is found beneath the AAIW stratum and in the Cape Basin lies below AAIW but above Antarctic Bottom Water (AABW). NADW at salinities >34.8psu and potential temperatures <3°C lies in a thick layer between 1000 and 3500m at the equator (Reid, 1989 in Shannon & Nelson, 1996) which spreads southwards from the North Atlantic. Flow of NADW into the Cape Basin is generally polewards along the continental margin although flow via the South Atlantic Current is possible (Shannon & Nelson, 1996).

Underlying NADW, the deepest layer in excess of 3800m, is AABW with salinities <34.82 psu and <1.4°C. AABW moves in a cyclonic circulation in the Cape Basin, with a poleward flow at the continental margin, the Walvis Ridge forms a barrier to the equatorward flow of AABW but leakage Cross the ridge has been documented (Shannon & Nelson, 1996).

1.3 Atmospheric Forcing

The winds in the Benguela are controlled by three mesoscale features: the South Atlantic Anticyclone/ High Pressure cell, eastward moving cyclones, and the pressure field over the African subcontinent. The South Atlantic High migrates seasonally over 6 degrees of latitude and 13 degrees of longitude (northwestwards in austral autumn and southeastwards in the spring), reaching its southern and northern extreme in February and May, respectively, while its western extreme is reached in August (Tyson, 1986 in Shannon & Nelson, 1996; Nelson & Hutchings, 1983).

Desert-like conditions in the coastal plains cause an interior thermal barrier to cross flow, this barrier causes the curved, anticyclonic flow associated with the South Atlantic High to move along the coast. The winds along the coast are therefore southeasterly in direction and "perennially favourable to upwelling" (Nelson & Hutchings, 1983, p. 339). The role of orography in previous studies listed in Jury, Kamstra and Taunton-Clark (1985), indicate that the orographic shearing of the low-level wind field over the northern part of the Cape Peninsula play a significant role in the alongshore variations in the coastal upwelling. Cole and Villacastin (2000) used satellite data to create sea surface temperature maps of the Benguela and found that strong upwelling activity occurs off headlands where upwelling-favourable winds are usually strongest and where the continental shelf is narrow allowing upwelled-waters to reaching close to the coast. The opposite occurs in bays and areas with a wide continental shelf.

The sequence of atmospheric events which lead to upwelling are depicted in the Figure 1.4(a-e) where low pressure cells are observed over a period of two weeks (Nelson & Hutchings, 1983).

Low pressure cells (cell *b* in Figure 1.4a) that form in the belt of westerlies between 35°S and 45°S ahead of planetary waves have associated cyclonic rotation and advect eastwards. As these cells move eastwards, they affect the wind field as far as the Olifants River and are modulated with an intensity that increases towards Cape Point, forcing upwelling in short scales of 3 to 10 days. In

addition, the South Atlantic high elongates, ridging round the continent (Figure 1.4b), this causes isobars to be compressed parallel to the coast resulting in the upwelling-favourable southeasterly winds, furthermore the wind flow undergoes dynamic compression and acceleration over the high mountains of the Cape Peninsula. With the arrival of the cyclonic system, cells of low pressure form at Lüderitz (coastal low). The South Atlantic High is weakened by the next approaching low pressure cell, c (Figure 1.4c) also the coastal low pressure cell begins to travel round the subcontinent as trapped waves and seem to be a precursor to the approach of these cyclonic systems (cell d). As the trapped wave moves along the coast upwelling is suppressed, relaxation of the wind at the centre of the system could cause inertial motions and shelf waves. The frontal system associated with the low, d causes winds from the southwest through to the northwest to the south (Figure 1.4d). These events are easily observed with the weakening of the modulation of the South Atlantic High in summer. In the winter the pulsation of the winds are weaker with the South Atlantic high migrating northwestwards and the frontal systems associated with the eastward moving lows penetrate the continent (Nelson & Hutchings, 1983; Shannon & Nelson, 1996).

Occasionally (observed in spring and autumn), a large interior high can form over the subcontinent and last 4 days leading to a 'berg wind' where dry adiabatically heated air flows off the plateau and upwelling is suppressed (Figure 1.4e) (Nelson & Hutchings, 1983; Shannon & Nelson, 1996).

Fennel (1999) summarises the wind as indicated by Boyd (1987), and Shannon and Nelson (1996), as highly seasonal with a maximum during spring and summer in the south while north of 31°S the wind displays a weaker seasonal variation and a permanent alongshore wind with a maximum during spring and summer and minimum in autumn.

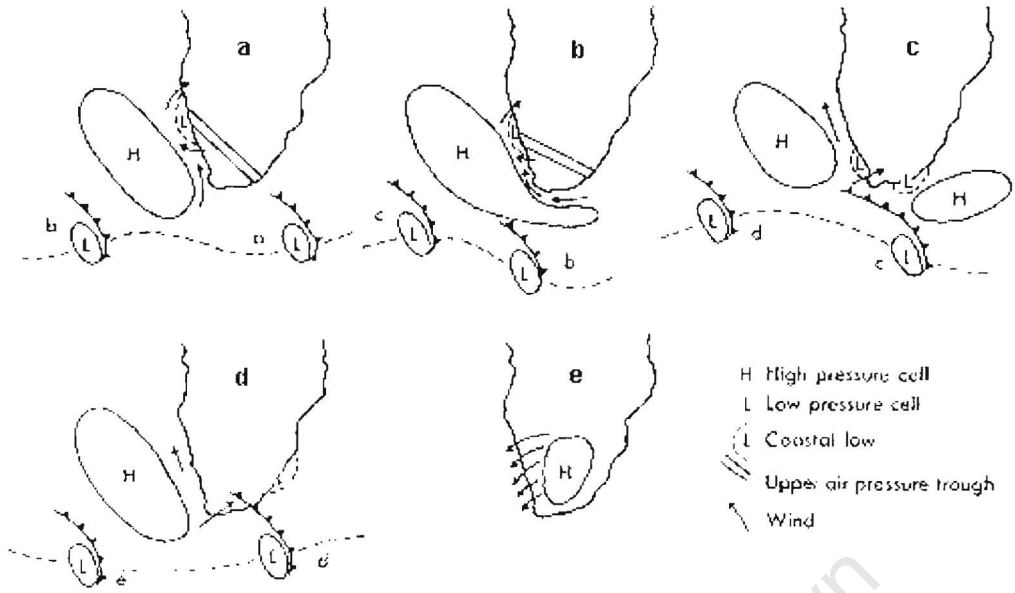

Figure 1.4(1-e): Cyclic weather conditions over the Benguela (typical of summer).

(a) South Atlantic High established. Coastal low at Lüderitz. Southerly winds at Cape Town.

(b) South Atlantic High ridging. Gale force winds at Cape Town. Coastal low moves south.

(c) South Atlantic High weakens. Northwest winds at Cape Town, following passage of coastal low.

(d) South Atlantic High strengthens. Southerly winds along west coast.

(e) Berg wind conditions. (Adapted from Nelson and Hutchings, 1983)

1.4 Features of the Benguela

The Benguela Upwelling System is comprised of many complex interactions, with a system of upwelling cells, fronts and filaments. In the following section, a brief overview is provided, in the aforementioned literature reviews of work on the Benguela these features have been covered in detail.

The northern boundary of the Benguela Upwelling System is indicated by the meeting of the poleward-flowing Angola Current and the equatorward-flowing Benguela at the Angola-Benguela frontal zone. The frontal zone is observed between 14 and 17°S as a persistent feature with a well-defined salinity and temperature to a depth of 50m but can be observed to 200m (Shannon & Nelson, 1996). The southern boundary of the Benguela Upwelling System is defined differently in various texts but can taken as either the Agulhas retroflection area (Shannon & Nelson, 1996; Nelson & Hutchings, 1983) or the southern extremity of upwelling (Shillington, 1998; Hart & Currie, 1960) which occurs south of Cape Town but occasionally extends onto the south coast at Cape Agulhas. In Hagen, Feistel, Agenbag and Ohde (2001), the southern boundary is described as a near-surface frontal system composed of the combination of Agulhas/ Indian water and Atlantic water

Upwelling occurs between these boundaries along the entire west coast of southern Africa, although the atmospheric systems that cause the necessary winds migrate seasonally, upwelling-favourable winds occur throughout most of the year. Upwelling is not uniform along the coast but occurs in localised regions, upwelling cells or centres. The semi-permanent upwelling cell at Lüderitz (27°S) is considered to divide the Benguela into northern and southern sections (Shannon & Nelson, 1996). Of relevance to this investigation is the Namaqualand upwelling cell centred at 30°S.

The spatial extent of upwelled water is identifiable by sea surface temperature anomalies, with upwelling associated with South Atlantic Central Water. Hart and Currie (1960 in Nelson & Hutchings, 1983) analysed temperature and salinity data from the Benguela and found that upwelled water originates between 200 and 300m. The offshore extent of upwelling, excluding major filaments, is between 150 and 250km. There are developed thermal fronts in the alongshore direction over much of the area between Cape Frio (18°S) and Cape Point (34°S). At certain areas such as South of Lüderitz, the fronts coincide forming a single front which follows the shelf-break (Skogen, 1999).

Hagen, *et al.* (2001), in a study to describe the annual and interannual variability in the Benguela upwelling regime by means of an absolute quantity used the 13° isotherm to describe the offshore extent of intense upwelling. Also indicated in the article is that this isotherm originates below the seasonal thermocline and tends to reach the surface close to shore during active upwelling.

Other "fronts" located in the Benguela include those which are zonally oriented and develop equatorward of the major upwelling cells, these "fronts" act as semi-permanent "discontinuities" within the upwelling system (Shannon & Nelson, 1996, p. 180).

In an introductory study by van Foreest, Shillington and Legeckis (1984), large frontal features in the Benguela current were explored using infrared satellite images. It was found that north of 30°S, features occur with a scale of hundreds of kilometres – extending from the continental shelf to the abyssal plane and form over a period of a week as well as decay with a similar period. South of 30°S, the features are described as resembling eddies with a scale of approximately 100km and located centrally over the shelf break. These features were suspected not to be the production of local effects of the bottom topography.

Upwelling tongues were found off Lüderitz at 200-400m moving slightly offshore in the summer, it was thus suggested that at regions similar to this (Lüderitz has a narrow shelf) upwelling might be enhanced by the bottom topography (Stander, 1964 in Nelson & Hutchings, 1983). In Nelson, Boyd, Agenbag and Duncombe-Rae (1998), the hydrography and upwelling filament off north-west Cape Town, its formation and the effect of shelf-waves on it was studied and discussed.

In an article by Jury (1988), aerial surveys were used to study the response to local topographic and meteorological forcings in relation to the upwelling cycle in three locations along Africa's west coast. For the west coast of Africa between 19 and 34 °S, the alongshore variability in coastal upwelling in response to a significantly varying wind stress field was emphasised. The upwelling region centred at 30°S (Namaqualand structure) was studied during various phases of upwelling and the relationship between the wind and an upwelling plume found off the region was discussed.

To the south of the Benguela Upwelling region, the influences of the Agulhas Current are apparent as seen by the temperature variations. Occasionally anticyclonic eddies are shed from the Agulhas retroflection region which move on to interact with Benguela filaments,

1.5 Shelf and Shelf-break circulation

In the review, by Shannon and Nelson (1996), unpublished knowledge of the authors on the circulation over the continental shelf are provided, comprehensive reference to the works of Boyd are made in addition to personal communication with Boyd. The following features of the Benguela Upwelling System are summarised (Shannon & Nelson, 1996, p. 188):

1. located in the western Agulhas Bank is a convergent NW-oriented current system which "funnels" into the West Coast jet current opposite the Cape Peninsula.
2. Flow inshore of the 500m isobath between Cape Town and Cape Columbine is described as "sluggish" due to the widening of the shelf. After this region the flow speeds up to 35cm/s.
3. Upwelling tongues are present in summer in the Cape Peninsula and Cape Columbine regions. Associated with each region is a narrow band of onshore flow north of each plume (Agenbag, 1992 in Shannon & Nelson, 1996).
4. A near-surface, southward current close inshore frequently appearing.

In Figure 1.5, the flow field of the surface and thermocline waters is shown, these flow fields include surface currents and the poleward undercurrent discussed below.

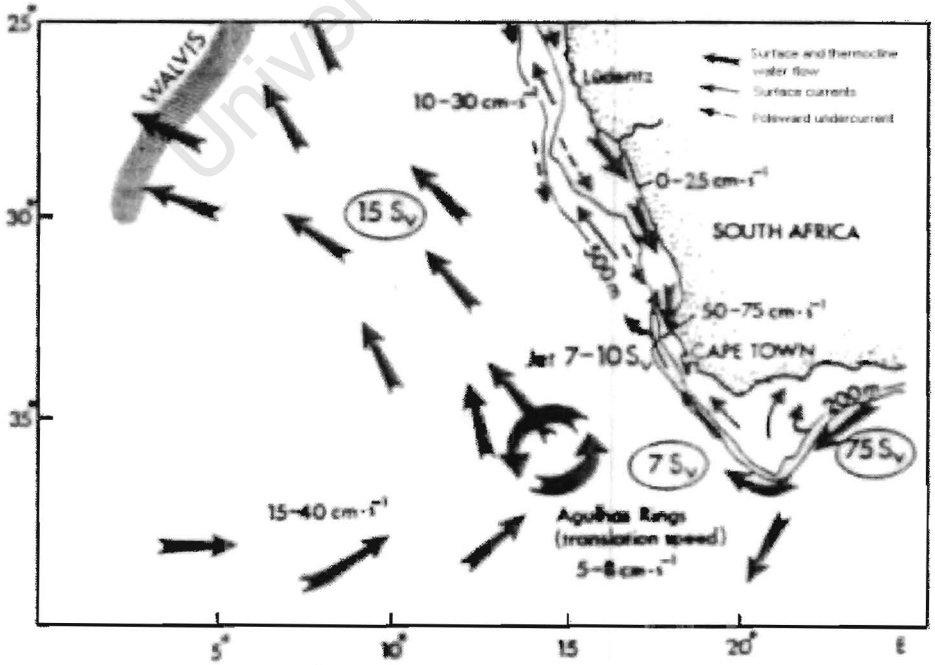

Figure 1.5: Schematic flow field of surface and thermocline waters
(Adapted from Stramma & Peterson, 1989 in Shannon & Nelson, 1996).

The poleward undercurrent is described by in Shillington (1998, p. 594) as "poleward flow of near-bottom water on the shelf". Hart and Currie (1960 in Nelson & Hutchings, 1983) initially found in their TS analysis evidence of a shelf-edge poleward undercurrent. This had been previously postulated as compensation to the vertical displacement of water and equatorward movement. Flowing under the equatorward surface flow, this poleward undercurrent is described as occurring with "varying strength and varying degrees of seasonal dependence", (Shannon & Nelson, 1996, p. 192).

Using current meters moored at various locations in the Cape Columbine - St Helena Bay region, the coastal current response to wind-forcing was investigated by Holden (1987) and the variability of the Benguela Current in time was shown to be modulated by the poleward undercurrent which, at Cape Columbine, was found with weak interannual variability at a depth of 150m. In addition, the study showed that for the period December 1982 and April 1986, mean southward flow was observed throughout the year. Further studies into the behaviour of the current in regions to the south and north of the current are discussed in Shannon and Nelson (1996) with many studies concerning the current off the narrow shelf off the Cape Peninsula (Bang & Andrews, 1974; Nelson & Polito, 1987).

Fennel (1999) applied a model to the Benguela Upwelling System and determined that the southward current can develop downwind of the surface current where the wind weakens and can reduce equatorward flow. In areas where the coastal current is weak, the counter current may exceed the current, inducing a mean poleward surface flow.

In Stramma and Peterson (1989), historical data was used to estimate the transport of water in the Benguela. The bulk of the Benguela Current is stated to flow northwestward after 32°S and then branch further at 28°S. Branching mainly westwards occurs with the topography until 15°S where the surface layer flows mainly to the west.

1.6 Benguela variability

Shillington (1998) describes several spatial and temporal scales associated with the Benguela Upwelling system. Obvious to upwelling is the effect of the wind which is forced by the atmospheric synoptic scale of 3 to 10 days and on a longer time scale of up to weeks. Seasonal changes in the wind patterns causes seasonal differences in the Benguela although Shillington (1998) references research by Nelson (1992) and Shannon *et al.* (1992) who showed that flow on the shelf, near Cape Columbine is dominated by a monthly signal with a seasonal signal not apparent.

An episodic event that occurs in the Benguela is the Benguela Niño (Shannon, Boyd, Brundrit & Taunton-Clark, 1986), where warm tropical water advects polewards along the coast influenced by anomalous wind stress and corresponding to decreased upwelling along the coast. Benguela Niño's introduce additional variability to the system, following a similar pattern to the Pacific's El Niño phenomenon in which warm tropical water advects polewards along the coast but appear independent of ENSO according to Philander (1990 in Shillington, 1998).

In a study by Cole and Villacastin (2000), satellite data was used to obtain the interannual trends and the large interannual differences in coastal SST. This was determined to be dependent of the events that occur during February to April as the other months are similar from year to year i.e. interannual trends are not affected by these months. The variability was determined to be principally due to SST variability between years rather than within the months themselves.

Blanke *et al.* (2002) discussed the role of wind stress on sea surface temperature anomalies by the comparison of simulations from a numerical model. Using various time scales of wind forcing the sensitivity of the coastal ocean was investigated by observing the response of sea surface temperatures to these forcings. The model was shown in this investigation to be able to reproduce features of the Benguela, with a maximum correlation between modelled and observed interannual SST over the continental shelf and Agulhas Bank.

As a basis to the investigation, climatological forcing, forcing that is consistent from year to year, was applied to the model and it was shown that mesoscale processes introduce variability on an interannual time scale. The various forcings consisted of monthly wind and real weekly wind fields and then a real weekly wind field combined with an alternative initial state. It was found that both wind and mesoscale activity played a role in introducing variability over the west coast upwelling region.

Shown in Figure 1.6, are the regions which are primarily driven by wind forcing and mesoscale activity play less of a role. An interesting region in Figure 1.6 is the feature off the shelf break (marked in red) which corresponds well to wind forcing. Low frequency variability is described as "the main contributor to the interannual SST variability " (Blanke *et al.*, 2002, pp. 3) while intra-monthly wind fluctuations play a large role at the shoreline as the ocean in this region immediately reflects the short-term perturbations in atmosphere.

SST anomalies over the shelf off the west coast (north of 29°S and downstream from St Helena Bay) was found to be attributable to local wind forcing. A region from 35 to 30°S was found not to respond to this forcing, instead this region appears to respond to features that have been advected from the south (Agulhas retroflection region) together with modifications from wind fluctuations.

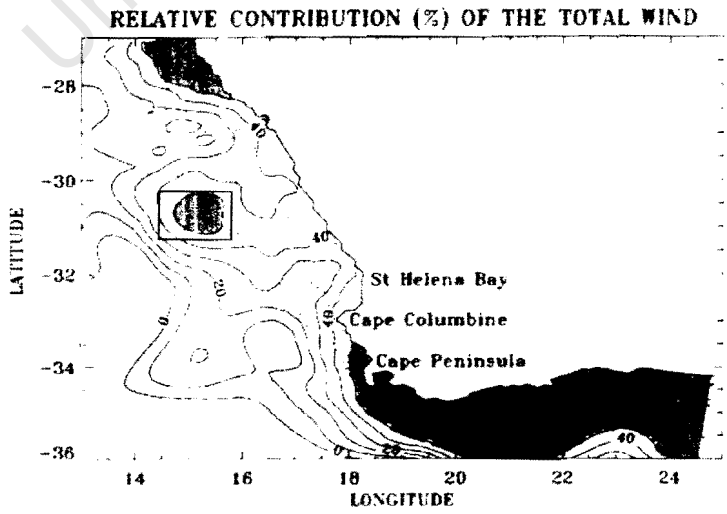

Figure 1.6: Percentage of wind contribution. Shaded areas indicate areas of significant contribution by winds (Blanke *et al.*, 2002).

1.7 General Hydrographic features of the shelf and slope

Studies have been performed in describing the structure and the processes involved in the ocean over the continental shelf and slope. In this brief section, three studies, although two occur on western boundary currents, are outlined together with their findings relevant to this investigation over the Benguela.

The Yucatan, like the Benguela, has both surface and opposing subsurface flow in addition to upwelling, by looking at this complex system, the processes and methods utilised by Merino (1997) could be compared to the Benguela. Using, hydrographic data from four cruises, Merino (1997) studied the structure of upwelling on the Yucatan shelf with emphasis on the mechanisms surrounding upwelling. Although the Yucatan is located in a western boundary region, it is considered as a "region of significant upwelling" (Merino, 1997, pp. 119) with upwelling appearing to follow a seasonal cycle. Upwelling in this region was postulated to be caused by bottom friction of the Yucatan Current against the slope of the shelf or even the combined effect of the current and its undercurrent. Since salinity variations on the shelf were minimal the temperature was used as a proxy for upwelling intensity and water mass structure. Observing the temperature distribution and pattern of isotherms cold water was seen to rise along the bottom boundary layer onto the continental shelf. Strong thermal gradients were also observed as well as the doming of isotherms to within 10 to 30m of the surface with upwelling not reaching the sea surface regularly. In addition, the existence of the slope countercurrent was confirmed, this countercurrent was observed, as spring proceeds to summer to occupy an increasingly larger section of the slope as its strength increased. This observation together with the apparent dependence of the upwelling on contact with the shelf suggested that it played a role in the cessation of the upwelling process.

Noble and Ramp (2000) used current-meter moorings over a time period of a year to investigate currents over the shelf and slope of California. It was found that the pattern of poleward flow showed no seasonal pattern and was not affected by either the local winds or local alongshore pressure gradient. The Californian undercurrent usually runs polewards lying seawards of the shelf break, inshore of

the equatorward California Current System. In the investigation, the mean flow over the shelf was found to be mainly poleward, with the higher speeds found toward the surface. There appeared to be, at most sites, no significant cross-slope flow. It was found that the alongshelf structure of the undercurrent was bimodal with both modes displaying a large horizontal extent offshore from the shelf break and reaching depths in excess of 800m. The first mode had a unidirectional flow pattern while the second was vertically sheared and strongest offshore. Also observed as part of the poleward current were strong jets which moved toward or away from the shelf break. These varying structures were believed to be attributed to the interaction between the current and the topography, with convergences in topography capable of generating undercurrent meanders which may form eddies. When the undercurrent is strong, rapid sheering of the topography can cause it to move offshore.

Lima, Garcia and Möller (1996) studied the southern Brazilian shelf using maritime weather reports and data from three hydrographic cruises. Circulation in this shelf region was found to display a seasonal pattern, with the wind-driven transport and geostrophic circulation producing a net flow to the south and offshore in summer and a reversal winter. In summer, the predominantly northwesterly winds cause upwelling by inducing offshore transport; this together with eddies that may cause shelf break upwelling result in enhanced upwelling in the region. In winter, opposite wind direction causes downwelling and thus offshore transport in the bottom layer of the shelf.

2. Modeling the Coastal Ocean

The oceans play a crucial role on earth including: the determining of earth's climatic conditions, as a food source, energy and mineral source, as well as in the defense and commerce needs of nations. Therefore a better understanding of the processes that govern the oceans are required. Since there are many limitations (cost and time) to the collection of *in situ* data from the ocean and the ocean interiors cannot be probed remotely, ocean models add to the understanding of these ocean processes (Kantha & Clayson, 2000).

Haidvogel and Beckmann (1998, p. 457) describe the coastal oceans as complex systems subject to "geometrical constraints of irregular coastlines and highly variable (steep and tall) bathymetry" and forcings by tides, wind and buoyancy factors on various temporal and spatial scales. These numerous factors result in various complex and physical processes. In a comparatively shallower region such as the coastal ocean, the effect of forcing at the surface and processes at the bottom are emphasized and models that incorporate the effect of the topography as well as includes reliable mixing physics must be used.

2.1 Previous Models of the Benguela

Previous models applied to simulate circulation and dynamics over the southern African coastal shelf and slope include the Princeton Ocean Model (POM), applied to the region between 46°S to 12°S and 4°E to 30°E (Penven *et al.*, 2001). It was found that this model, although simulating large-scale features, was too coarse to resolve mesoscale patterns in the circulation in the applied area.

2.2 Description of ROMS

The three-dimensional hydrodynamic model ROMS (Regional Ocean Model System) applied to the southern Benguela was developed at Rutgers University and the University of California at Los Angeles. ROMS is described by Penven *et al*, (2001, p. 472) as " a community model shared by a large user group around the world, with application ranging from the study of entire ocean basins to coastal subregions." ROMS is part of a hierarchy of terrain-following models incorporating SPEM (semi-spectral primitive equation model) and SCRUM (S-coordinate Rutgers University Model) which is an improvement of the former, in turn ROMS is an evolution of SCRUM.

ROMS was applied to the southern Benguela as part of the VIBES (Viability of exploited pelagic fish resources in the Benguela Ecosystems in relation to the environmental and Spatial aspects) programme which aimed to obtain knowledge on the processes that effect the recruitment of fish in the Benguela (Penven *et al.*, 2001). ROMS therefore provided the numerical tool to simulate the dynamics of the circulation in the relevant regions. A thorough description of the numerical model is provided in "A numerical study of the Southern Benguela circulation with an application to fish recruitment" by Penven (2000).

The model domain covers the coasts from Cape St. Francis on the South coast to Lüderitz on the West Coast which forms the Eastern and Northern boundary to the open ocean, respectively - boundaries occurring where the shelf is at its narrowest. In effect, the pie-shaped grid covers the southwestern corner of southern Africa from 40°S to 28°S and from 10°E to 24°E (Figure 2.1). The offshore boundary is placed on the ocean plane about 300km from the tip of the Agulhas Bank. The domain therefore ranges from 1300km in length at the coast (inner radius) to 2240km offshore (outer radius) with a width of 750km. The model used in this investigation is considered a medium resolution model, linearly ranging from 9km at the coast to 16km offshore (Penven, 2000).

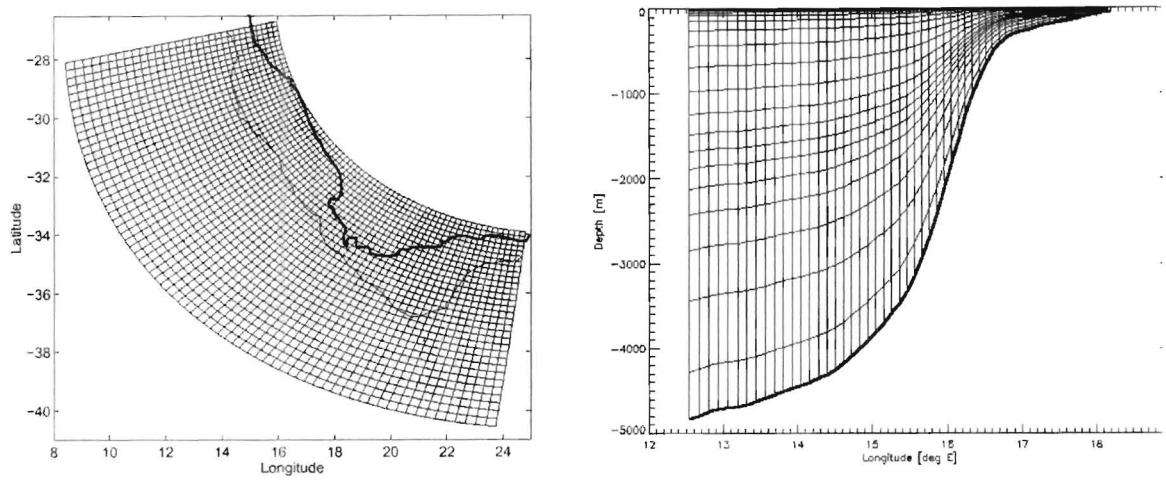

Figure 2.1: The ROMS spatial grid (left) (Penven *et al.*, 2001) and the vertical grid (right) over the southern Benguela.

The grid covering the Benguela was created with the following considerations:

- That the domain covered must be large enough to incorporate the larger features responsible for the transport of eggs and larvae e.g. upwelling filaments, Agulhas retroflection.
- The domain must also be small enough to keep computational costs to a reasonable amount yet keep resolution high.
- The open boundaries should cross the current at 90 degrees and be placed where current velocities and variability are minimum. In addition, along-boundary current should be avoided by keeping the topographic gradient perpendicular to the boundary as small as possible (Penduff, 1998 in Penven 2001).

In order to satisfy the above criteria for the domain, the grid was constructed to follow "the arc of a circle", lying over the Southwest corner of Africa and maintaining identical resolution in the ξ and η directions (horizontal curvilinear coordinates corresponding to a transformed x and y, respectively). This method aims to minimise the number of points falling over the irregular-coastlined land (masked points) that do not assist in the computation of the solution.

The topography was derived from the ETOPO2 dataset and is set to configure to the model resolution. Due to the pressure gradient scheme much of the rapidly varying topography has been filtered out, especially where the topography is steep, thus features such as the Cape Canyon has been filtered out. In addition, the filtering has removed the narrow shelf adjacent to the Cape Peninsula. A specific open boundary scheme has to be added to the model at the east boundary as there is a strong influence of the Agulhas Current.

The vertical coordinate system used by ROMS is based on the sigma coordinate system as opposed to the more traditional z coordinate system using geopotential levels. The sigma coordinate system follows the bottom contour of the topography and can incorporate a bottom boundary layer as well as a surface boundary layer; in addition, there is a consistent number of coordinate surfaces independent of the depth of the water column The coastal ocean, especially over the shelf, is shallower than the open ocean and therefore the effects of the surface, vertical dynamics and the bottom boundary layer/ bathymetry must be considered (Kantha & Clayson, 2000). There are 20 vertical layers in the model most of which occur at the surface in order to maintain a good resolution of the depths at which most biological components are found as well as where most physical variability occurs. The number of layers was found to be optimal as increasing the layers to increase resolution along the bottom did not result in a "significant improvement of the solution." (Penven, 2000, p. 76).

The atmospheric forcing applied to the model is based on monthly climatologies derived from the Comprehensive Ocean-Atmosphere Data Set (COADS) (Da Silva, Young & Levitus, 1994 in Penven, 2000). An implicit active radiative boundary scheme which is forced by the seasonal climatology computed from the AGAPE basin-scale ocean model, is applied to the three lateral boundaries facing the open ocean. The effect of the Agulhas Current that affects the southeast corner of the domain has been considered and was compensating by the addition of a condition for the depth-integrated transport originally considered for tidal models.

2.3 Limitations of ROMS

When the model is applied to a steeply changing topography such as the continental slope, a pressure gradient error can occur. The continental slope is therefore poorly represented in these models (Kantha & Clayson, 2000).

In sigma coordinate models, the pressure gradient term is split into an "along-coordinate surface" component and a "hydrostatic correction" involving the gradient of pressure along a constant σ-surface and the gradient of the bottom topography, respectively. A pressure gradient error can develop near steep topography, as the above terms become large with similar magnitudes but opposite signs, resulting in an erroneous total pressure gradient force throughout the water column (Haney, 1991 and Haidvogel and Beckmann, 1998).

2.4 Model Applications

Regional models applied to a coastal oceans assist in the understanding of the "formation, exchange, spreading and mixing of water masses in realistic geometries and under typical or extreme forcing situations", (Haidvogel & Beckmann, 1998, p. 464). Specifically applied to certain regions, models have been used to simulate, hindcast and forecast coastal flows. Recently coastal models are used as the basis for coupled studies of biogeochemical interactions and used for ecological modeling.

3. Methodology

3.1 Data

The data used in this study was obtained from output derived from numerical model simulations. Using the Regional Ocean Modeling System (ROMS), a medium-resolution, pie-shaped grid was applied to the southern Benguela (40°S to 28°S and 10°E to 24°E) with resolution linearly ranging from 9km at the coast to 16km offshore (Penven, 2000).

The model runs were forced by wind stress product from ERS1/2 satellites consisting of a weekly 1° by 1° gridded time series from August 1991 to January 2001. Blanke *et al.* (2002) found this satellite data of the wind to correspond well with *in situ* anemometer measurements at Cape Columbine (32°50' S) on the West Coast, with a correlation coefficient of 0.8. In addition, the satellite data was found to be one-third larger than the local measurement explained as the effect of orography experienced by the anemometer. Despite differences in measurements which were attributed to the inherent characteristics of both measurement techniques, the product was found to be applicable to the southern Benguela.

The model was forced by truly observed weekly winds (Run C) to obtain realistic data. The output of the model runs for each grid point consist of 2-day values of which there are 15 per month for the period corresponding to August 1991 to January 2001.

In Blanke *et al.* (2002), an area above the shelf break that corresponded well with wind forcing, was observed off the west coast. The transect under investigation was selected as it passes through this aforementioned area and samples the hydrography of this region together with the surrounding waters. In addition it passes through the regions under intense investigation by as it incorporates the Ibhubeysi Gas Field which is considered an important future source of energy for South Africa. The transect incorporated the offshore extent of the poleward

undercurrent as well as included the shelf break and its adjacent area. The transect extended from the coast at 29.6909°S, 17.0673°E to 31.0650°S, 14.5109°E, spanning about 290km and reaching a maximum depth of 2125m (Figure 3.2). As part of this vertical virtual study, four "moorings" were chosen, at the coast, mid shelf, at the shelf-break and over the continental slope to investigate the temporal characteristics of the transect (Figure 2.2). The details of these "moorings" are described in Table 2.1.

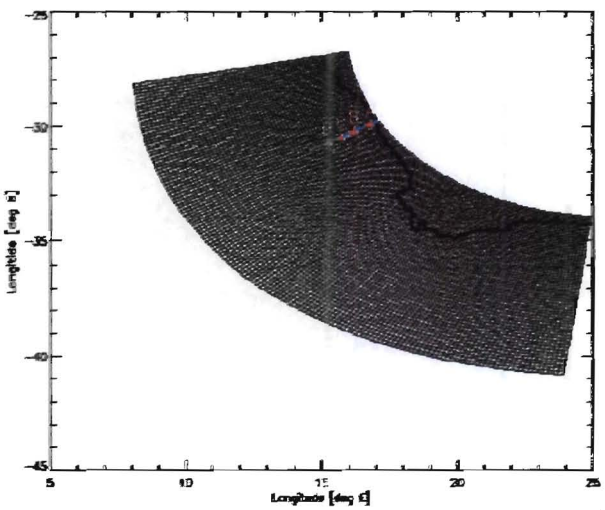

Figure 3.1: Horizontal grid showing transect in blue and the position of the four moorings (red triangles).

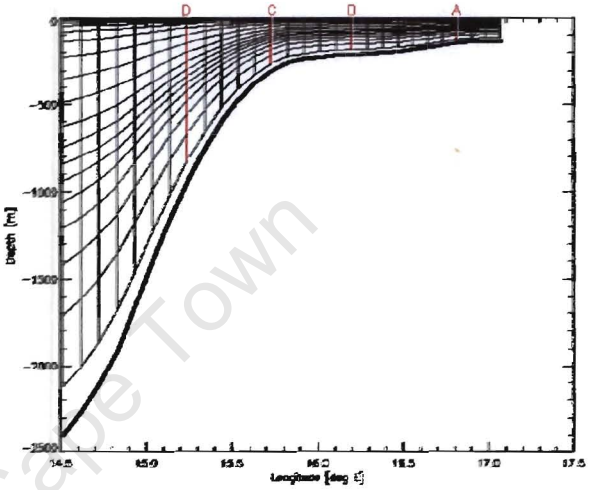

Figure 3.2: Vertical grid of the transect, with the four moorings shown in blue.

Table 3.1: Description of the moorings

Mooring	Latitude (°S)	Longitude (°E)	Depth of Bathymetry (m)
A	29.8221	16.8157	134.063
B	30.1420	16.1990	200.311
C	30.3830	15.7317	286.460
D	30.6348	15.2408	922.956

Jury and Courtney (1995), found that in the central Benguela, sea surface temperature (SST) variability is driven by local upwelling. Therefore SST is of particular interest to this investigation as it reveals the physical manifestation of the ocean's response to wind forcing. In addition, cross-shore (u) and alongshore (v) current speeds are considered as they yield an indication of the processes and structures that are found in the region from the shelf break toward the coast. As the location of the grid points of both u and v current speeds varied from that of temperature, the currents were linearly interpolated to hold for the same location as the temperature

3.2 Data Processing

The independent software programme Interactive Data Language (IDL) was used to process and visualise the data. The monthly climatology was obtained by averaging the 2-day data for each grid point over the whole month and then averaging for the nine/ ten years of data. By plotting the monthly climatology, a steady picture of the region is obtained by levelling out highly variable structures, both spatially and temporally. In addition, currents were subjected to spatial smoothing with a boxcar average. An oceanic response every two days from wind forcing may result in "noise", thus with smoothing out the plots constant spatial and temporal patterns become more apparent. For each vertical section the variability of the data for each grid point was indicated by the standard deviation. Due to the nature of the sigma coordinate levels the array was not regular and the each data point had to be plotted at its individual location.

The contour intervals were user-defined and differed for each parameter, the colour scheme is consistent for each parameter but are not comparable as it uses the range of the parameter. In addition, in order to compare features within a parameter, the contour interval may differ for positive and negative flow. The colour is not necessary but is used rather to aid the visualisation of the specific variables. For the currents, the $0cm.s^{-1}$ isotachs have been highlighted in bold as to show the transition between opposing flows. In addition, positive flow for this model is south and west, current direction is stated for each graph.

For the Hovmöller plot, temperature and currents were interpolated at 1m intervals for the required depth of 50m, using the new levels the average was obtained for the upper 50m of the ocean.

4. Results

Vertical Temperature Distribution

Figures 4.1 (a-l) display the vertical climatology of monthly temperature for the transect from the coast at 17°E to 14.5°E, with the isotherms spaced at 1°C intervals. It was observed that surface waters over the slope were warmer over the summer months (December to February) and reached an average 20°C as in January and February (4.1a & b). In contrast, the winter months (June to August), temperatures are cooler at 16°C as in July and August (4.1 g & h). The seasons in between displayed a transition state between the two. Common to all months was the shoaling of isotherms over the shelf. As observed in the summer months, the coolest waters to reach the shelf were 11°C, upwelling from a depth of approximately 300m. In winter, the 11°C waters seldom reach the shelf, although the water may already be found on the shelf.

All isotherms in the upper 300m were positively sloped toward the shelf and surface. This could both be indicative of local coastal upwelling occurring throughout the year or associated with the broad equatorward flow of the Benguela Current under geostrophic conditions. The steep inclination of isotherms at the coast coupled with the compression of isotherms during summer displayed that upwelling varied in intensity and was seasonal for this region. These features confirm expectations of the classical view of upwelling: warmer temperatures offshore due to solar heating but increased wind stress introducing cold upwelled waters inshore over the shelf and the opposite case in winter with less heating and decreased upwelling.

The water situated along the continental slope below 500m was consistently stratified with the 8°C isotherm located at this depth and below 4 to 7°C water in layers of 100m thickness. The bottom layer was comprised of a 700m thick layer of 2°C underlying a 400m thick layer of 3°C water. The minimum above slope temperature of the climatology was 16°C and found at the surface during winter.

Contrary to upwelling, this water did not appear to originate at depth and was observed to extend eastward up to 15.9 °E offshore in mid-winter, July (Figure 4.1g). In summer, with surface warming, the 16°C water lay at a depth of around 100m over the slope, with upwelling at the coast the 16°C isotherm penetrates the surface around 17 °E mid-summer, reaching far closer to the coast than during winter.

At the shelf break at depths between 300 and 400m, the isotherms intersecting the region were displaced vertically downward. This is indicative of the poleward undercurrent. The downward gradient of the surrounding isotherms varied throughout the year being minimal in summer. As previously discussed, there were remnants of 11°C water on the shelf even though the isotherm did not reach the shelf during winter, during which diminished upwelling still occurred. The shelf-presence of this water combined with the downward displacement of the associated isotherm suggested that the poleward undercurrent plays a role in this process, possibly interrupting the flow of water upwelling onto the shelf as discussed by Merino (1997) in respect to the Yucatan shelf.

Figures 4.2 (a-l) display the standard deviation of temperature of the transect mapped in the vertical, with the standard deviation isolines spaced at 0.2°C intervals. The standard deviation gives an indication of the variability of the section, with higher standard deviations implying a larger range of temperatures and thus larger variability. Predictably, spring / summer (November to March), displayed maximum variability (standard deviation up to 1.6°C) in two regions, offshore over the continental slope centred at a depth of 100m around 14.5 °E and at the coast above a 50m depth. During autumn and winter, maximum variability occurred in two concentric areas: close to the coast in the upper 100m (17.2 °E) and over the shelf break centred at a depth of 100m, both of which reached a maximum variability of 1.6°C.

Below 1000m there very little variability was observed in the temperature sections, the water at depth remained highly stratified and consistent throughout the year. In addition, the shelf bottom was observed to be a region of low variability.

Close to the coast throughout the year, the temperature variability in the upper 300m appeared to follow the pattern of upwelling found in the temperature sections, suggesting upwelling consistently occurred at the coast displaying temperature fluctuations in intra-monthly time scales.

This pattern of sloping isolines toward the coast was not repeated over the shelf break. Instead, a distinct doming pattern was observed in this region, particularly in February and March. This suggests that a certain stable feature occurred over the shelf break, since further onshore variability resumed its increasing pattern, the dome could possibly indicate the spatial extent of this feature. Variability in these regions was maximum for summer and the surrounding months as discussed previously. In winter, the offshore variability did not appear to be significant but the coastal variability showed a pattern similar to upwelling, with isotherms tilting upwards. This possibly suggests that the isotherms and spatial distribution of upwelled waters close to the coast are quite variable.

In summary of the above, features introducing variability to the section were: two globular regions of maximum variability, one in the surface waters over the shelf at the coast, one over the continental slope and a feature causing doming over the shelf break.

The temperature sections alone, were not sufficient to describe the relationship between these features, but the large variability at the surface near the coast appeared to be consistent for all months of the year for this transect, with maximum occurring during summer when wind stress is generally maximum.

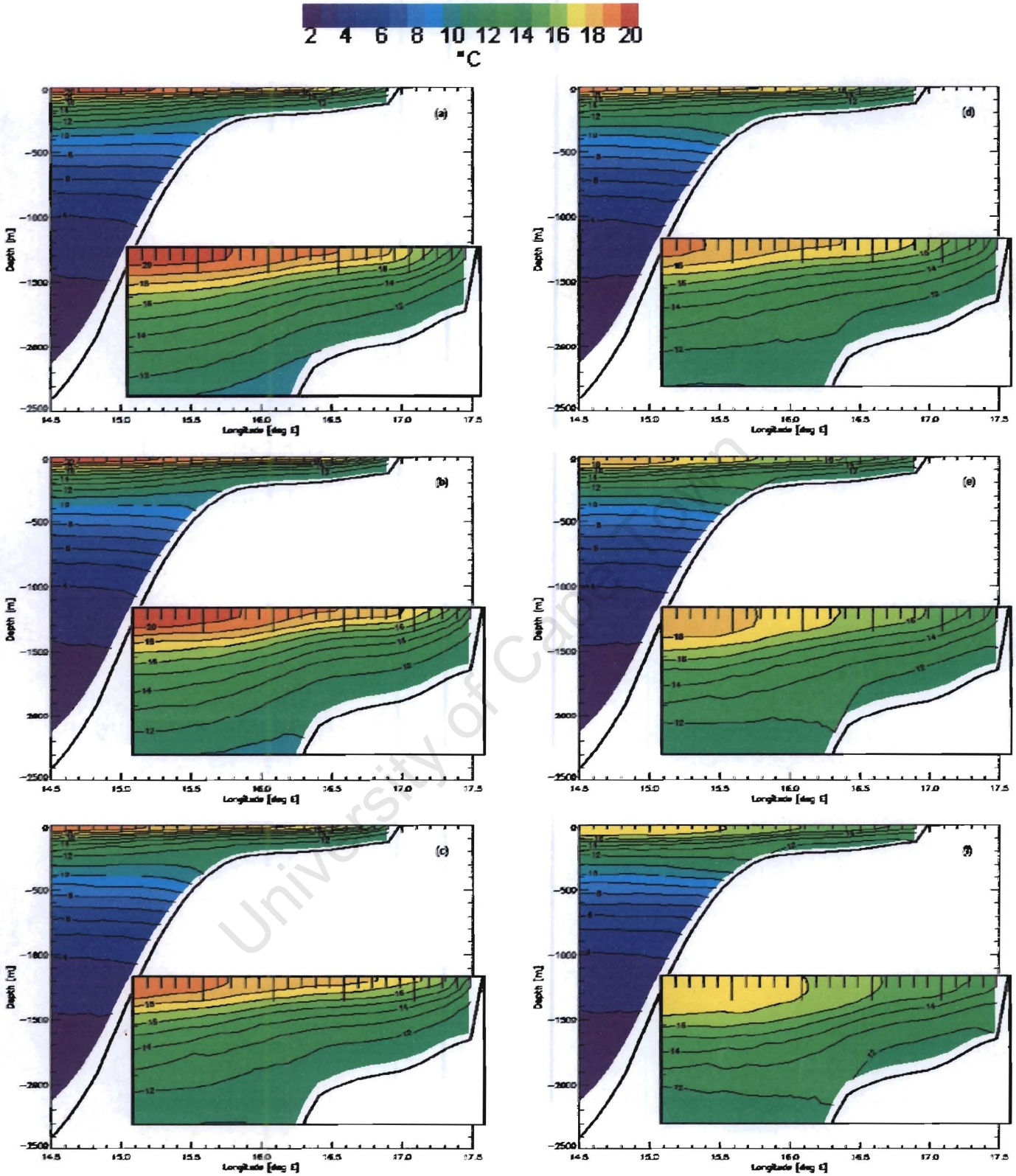

Figure 4.1 (a - f): Vertical section of temperature (°C) monthly climatology (January – June).
Inset: Zoom of upper 300m of section.

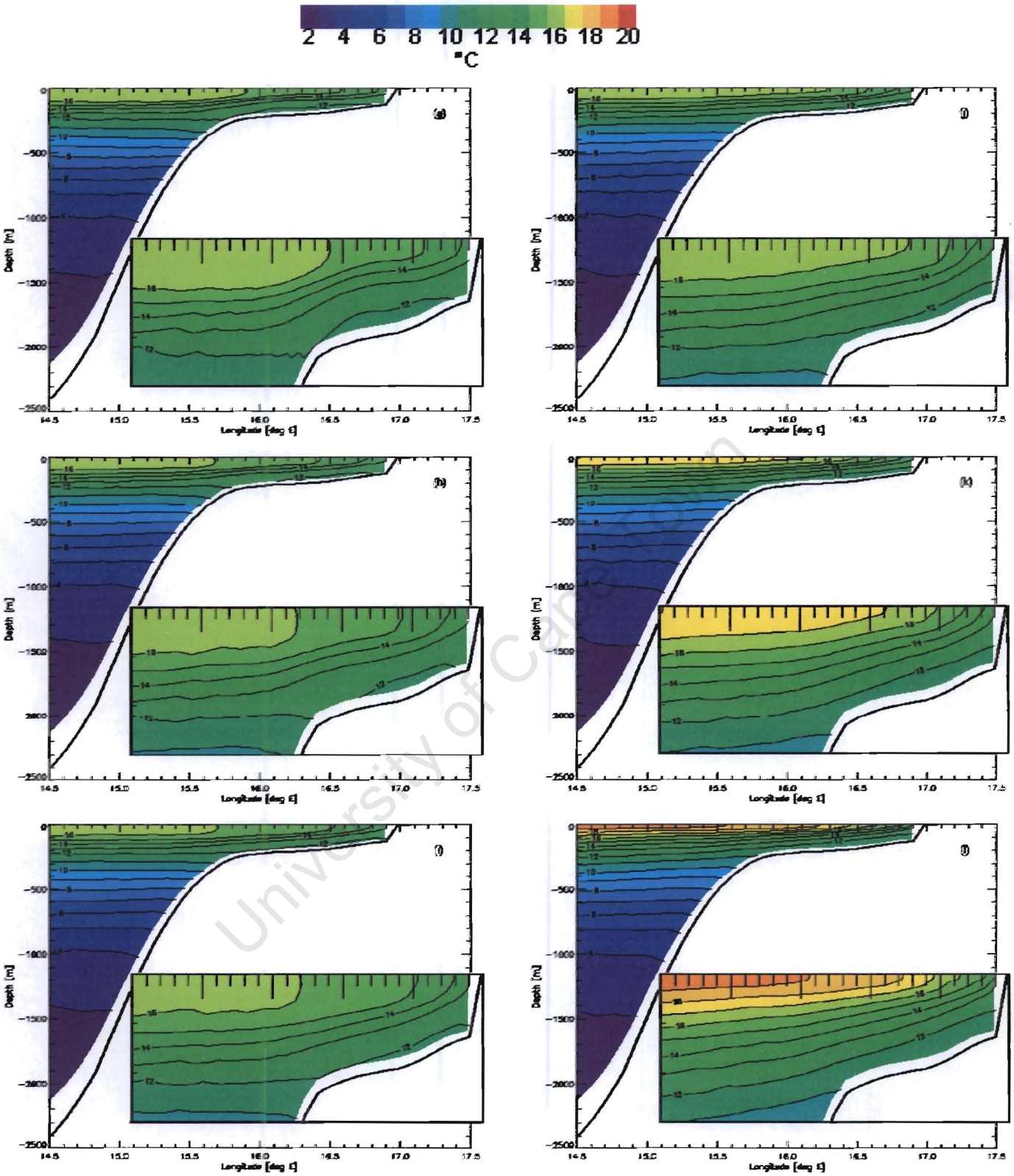

Figure 4.1 (g - l): Vertical section of temperature (°C) monthly climatology (July – December).
Inset: Zoom of upper 300m of section.

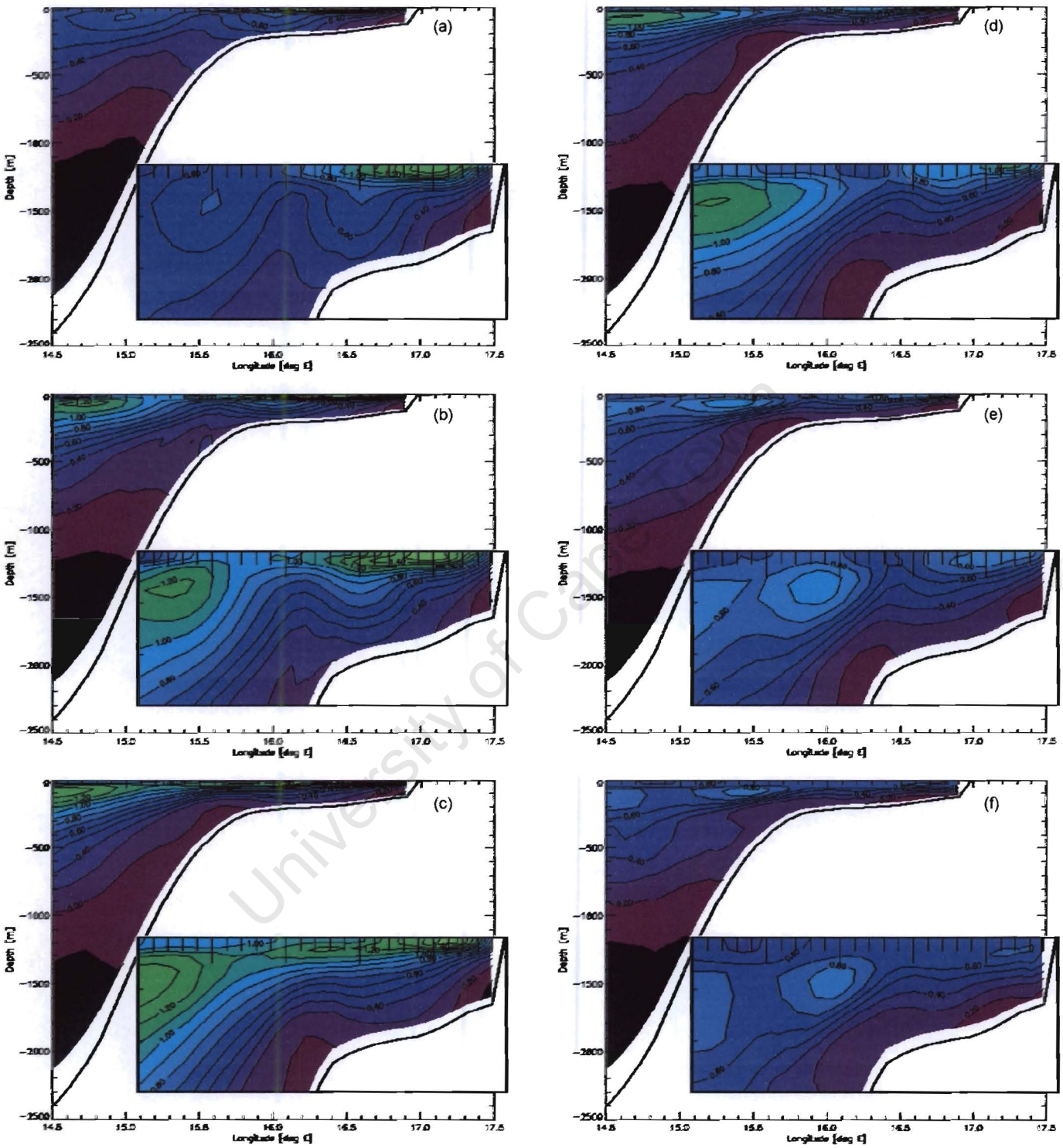

Figure 4.2(a - f): Vertical section of smoothed temperature standard deviation (°C) monthly climatology (January - June).
Inset: Zoom of upper 300m of section.

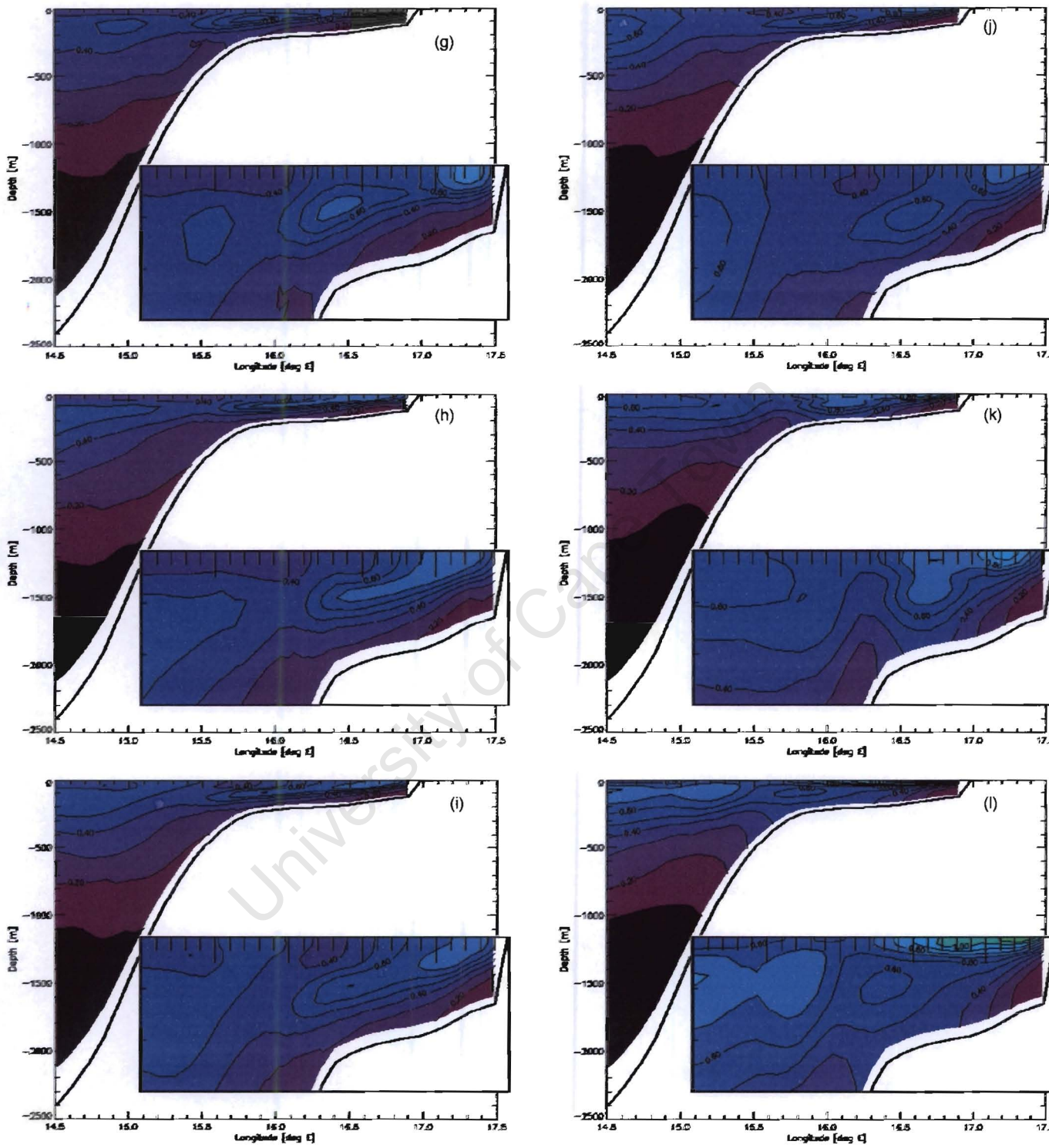

Figure 4.2(g - l): Vertical section of smoothed temperature standard deviation (°C) monthly climatology (July – December).
Inset: Zoom of upper 300m of section.

Cross-shore Current (u)

General observation of the climatology of cross-shore current (Figure 4.3 a-l) revealed that flow was mostly offshore, although a mid-depth layer of onshore water penetrated the shelf and reached the coast, having a maximum spatial distribution over the shelf in February through May.

As observed in the enlarged views of the cross-shore current, Figure 4.3 (a-l inset), the water in the upper 300m flowed mostly offshore. From December through May, there was an observable onshore flow of water onto the shelf at the bottom with a maximum spatial distribution in February. This onshore flow was easily identified by locating the $0cm.s^{-1}$ isotach, which separated the opposing flows. Onshore flow of water was observed to occur in a significant motion of water from between depths of 200 to 1000m and irregularly from even deeper down the water column. This onshore flow entered the shelf at mid-depth around 500m, and the thickness of this layer varied by month. The flow of water along the bottom appeared to be consistent with upwelling, where water at the surface moves primarily offshore to be replenished by water moving along the bottom from depth. In all months, the onshore isotachs did not penetrate the surface, but shoaled considerably toward the coast.

At the surface, there were two regions which display a core of intense offshore flow, probably in response to the wind: one over the slope which migrated with varying month and one at the coast. In winter when the wind stress has decreased, there appeared to be only one flow. The surface Ekman transport observed as the offshore flow probably responds to water from depth upwelling causing the doming of isotachs which causes a rift in the offshore flow resulting in two apparent cores.

At the surface, offshore flow of water was at a maximum over the continental slope in summer and moved eastward where it lay over the shelf break and shelf in winter. This reflects the difference of the seasonal winds. Weakened winds in winter imply weakened offshore Ekman transport of waters observed as weaker surface flow.

In January (Figure 4.3a) a core of offshore flow over the shelf break reaching speeds in excess of 18cm.s^{-1} was observed, probably in response to the increased wind stress in summer. With depth, this speed was observed to abruptly drop to 0cm.s^{-1} near 300m, where water flowing in the opposite direction was encountered. In an opposing flow to the surface water, water from depth moved up and along the shelf from 1000m toward the shelf at speeds less than 1cm.s^{-1}. This water was observed to only move to mid-shelf.

In February the core of the offshore flow was observed to move westward combined with a drop in speed to 14cm.s^{-1} at the surface. The depth of the offshore-flowing layer decreased to 200m over the slope and to about 50m at the coast. Increased upwelling was readily observed due to the thickness of the upwelling layer together with the increase in speed (up to 2cm.s^{-1}). In addition, the flow reached the coast.

March reflected similar conditions to February with the exception of the upwelling layer not originating from the large depths as before. In April through November offshore flow decreased in intensity (6-10cm.s^{-1}) and the cores of maximum speed moved further inshore together with an increased offshore layer depth. In June and July the breakdown of upwelling was observed although some water remained on the shelf. From August to November there was onshore-moving water at depth as well as at the coast but the former water did not reach the shelf. In November, intensity of the offshore flow increased until December when upwelling resumed.

General observation of Figures 4.4 (a-l), the standard deviation of cross-shore current of the transect in the vertical, with the isolines spaced at 1cm.s^{-1} intervals, showed that the cross-shore current was highly variable. Maximum variability occurred at the surface as expected since this is the region directly affected by the highly variable wind stress. Water at depths below 1000m displayed minimal variability as these regions were beyond the influence of surface processes.

The variability displayed a similar pattern to that of the cross-shore current, with "cores" of high variability at the surface coinciding in areas with maximum cross-shore current. As the transect progressed onshore, there was a positive displacement of the variability isolines. In certain months the doming of these isolines over the shelf break became apparent, this indicated an area where there was a consistent response to external forcing, hence the decrease in variability in this region.

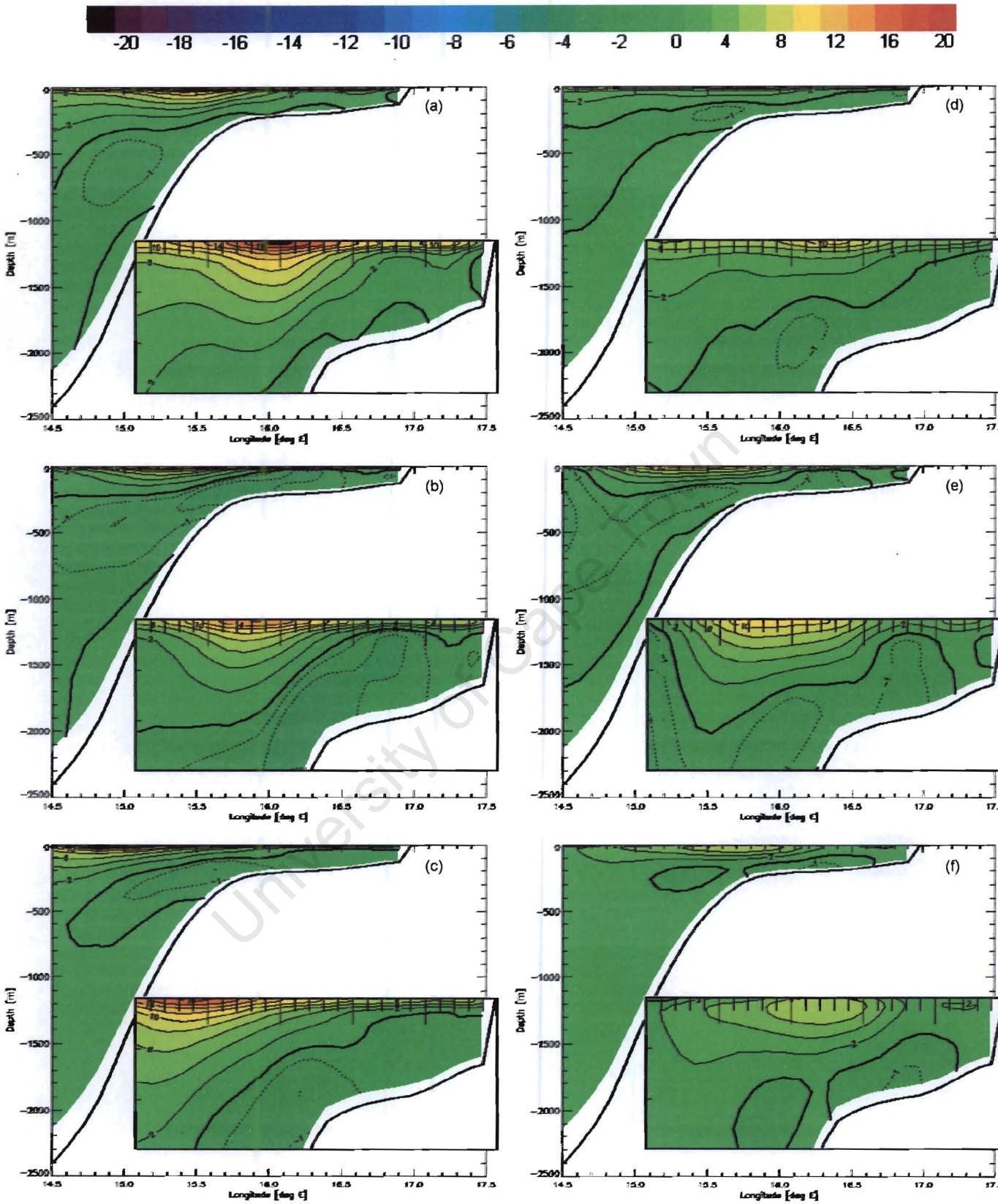

Figure 4.3 (a - f): Vertical section of the monthly climatology of cross-shore current ($cm.s^{-1}$) for the transect (January – June).
Solid line = offshore flow, dashed line = onshore flow. Bold line = O $cm.s^{-1}$ isotach.
Inset: Zoom of upper 300m of section.

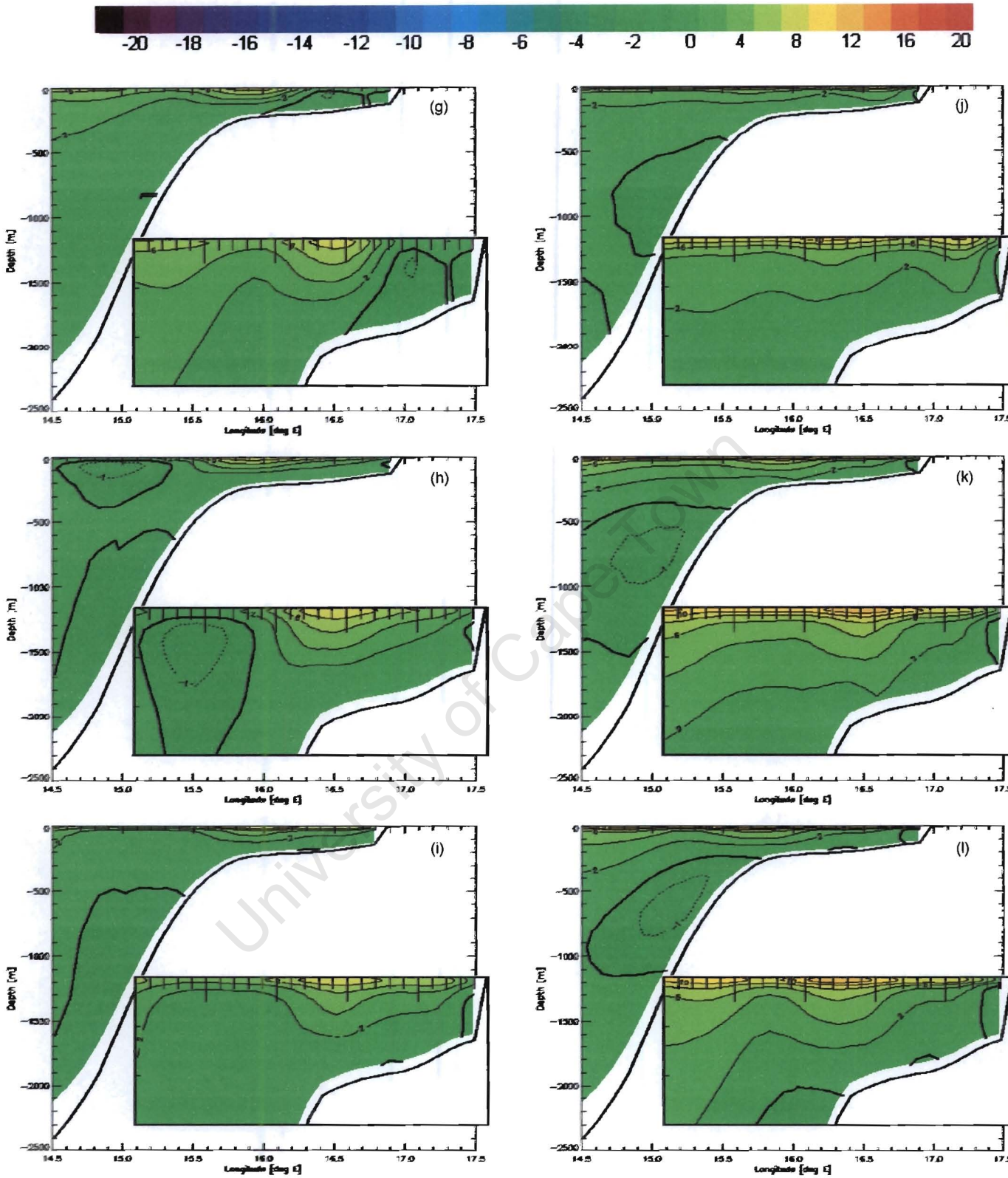

Figure 4.3 (g - l): Vertical section of the monthly climatology of cross-shore current ($cm.s^{-1}$) for the transect (July – December).
Solid line = offshore flow, dashed line = onshore flow. Bold line = 0 $cm.s^{-1}$ isotach.
Inset: Zoom of upper 300m of section.

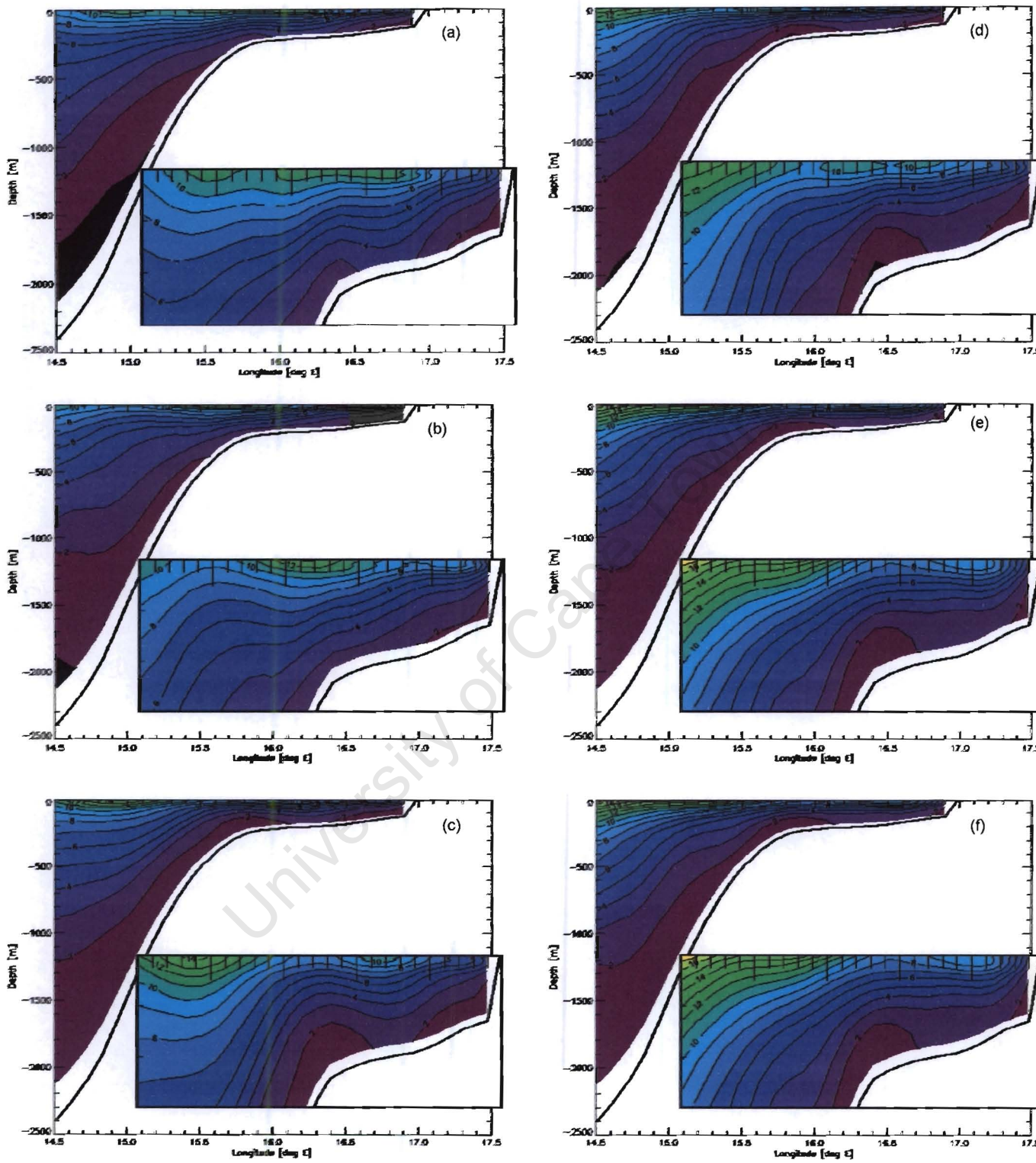

Figure 4.4 (a - f): Vertical section of the standard deviation of cross-shore current ($cm.s^{-1}$) for the transect (January – June).
Inset: Zoom of upper 300m of section.

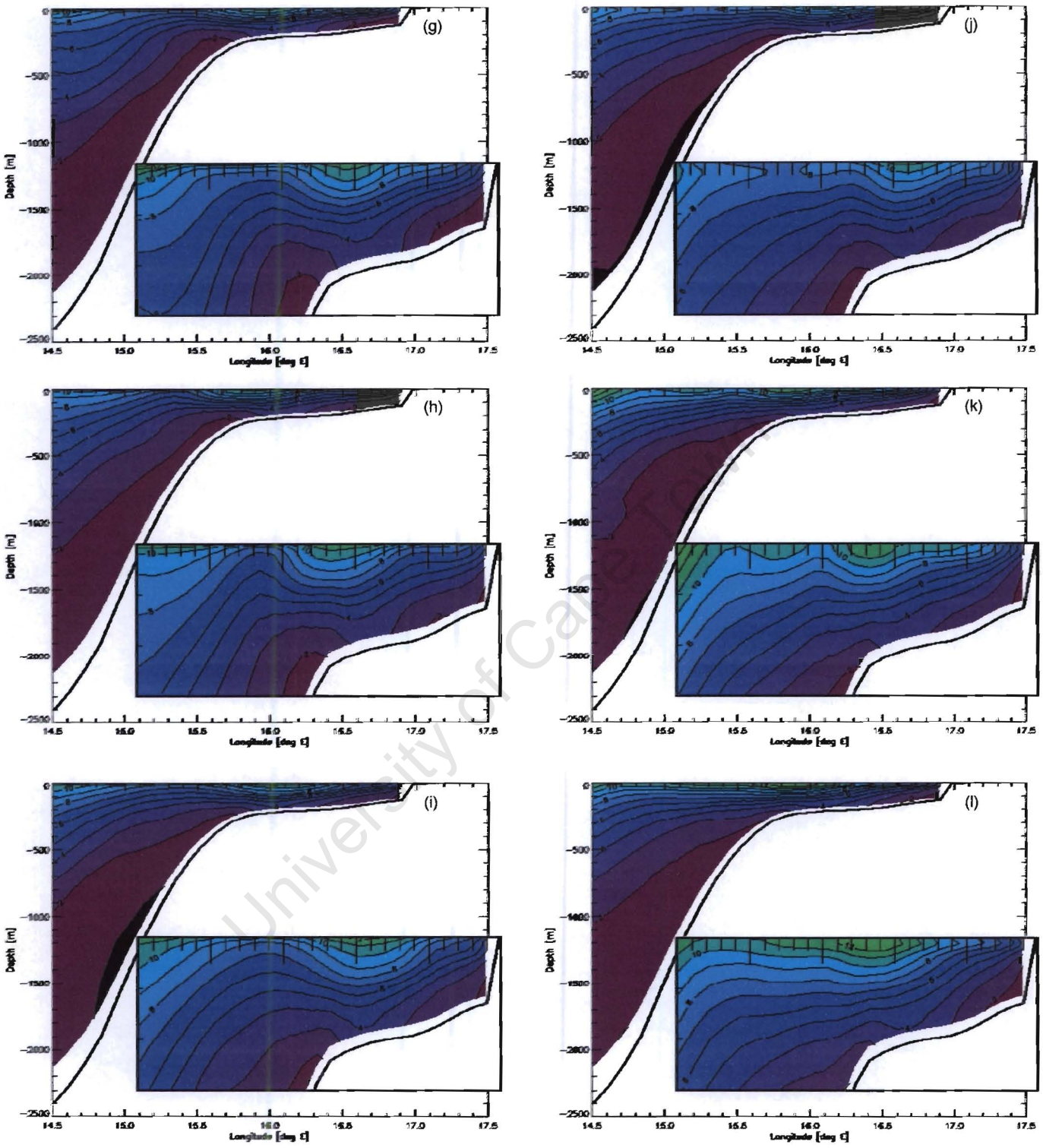

Figure 4.4 (g - l): Vertical section of the standard deviation of cross-shore current ($cm.s^{-1}$) for the transect (July – December).
Inset: Zoom of upper 300m of section.

Alongshore Current (v)

General observation of the climatology of alongshore current (Figure 4.5 a-l), shows four areas of flow: positive, equatorward surface flow at the coast; equatorward, surface flow over the shelf-break; a negative, poleward flow at 200m depth over the shelf-break and a negative, bottom, poleward flow at the coast. There was no apparent seasonality to the surface flows, if alongshore wind stress influenced this flow there would be a more seasonal reaction pattern.

Adjacent to the coast (east of 17°E), equatorward flow at the surface was apparent throughout the year, reaching up to 20cms^{-1} during summer. Minimum current speed for this flow occurred in winter where maximum speeds at the surface range from 8-12cm.s^{-1}. Over the continental slope a larger but more variable flow occurred, possibly coinciding with the core flow of Benguela Current. When the currents relaxed, for example in September, there was no apparent distinction between the two flows. These two surface currents appeared to vary in intensity throughout the year, spatially varying from deep and narrow to shallow and broad, though no relationship between the two was apparent. In Stramma and Peterson (1989), flow north of 28°S is described to branch. Therefore, the two equatorward flows at the surface could be consistent with this description.

A negative poleward current was observed between the Benguela Current, above the shelf break, below, possibly corresponding to the Benguela undercurrent. This poleward flow was observed in all months to be in constant contact with the shelf break. Flow of the poleward current from January to April was fixed around a concentric core with maximum speed of 5cm.s^{-1} (observed in February and March). From May through September the poleward flow shedded its core shape and extended onto the whole shelf reaching the coast in a bottom topography-hugging layer. In June this flow appeared to split into the poleward flowing shelf-bottom layer and a large, slow current offshore over the continental slope. The off-shelf part of the poleward current at this stage, joined with a poleward flow that encompassed most of the water column at 14.5°E.

By following the poleward-flowing layer (below the 0cm.s^{-1} isotach), spatially smaller flow on the shelf was observed in the 3 months proceeding June, remnant of the splitting of the poleward undercurrent observed in June. In addition, the core of the poleward undercurrent over the shelf-break was not observed for these months. September revealed only poleward flow hugging the continental slope and extending to depth. This poleward flow on the shelf was small in magnitude and reached a maximum of 1cm.s^{-1} in September. In October and November (Figure 4.5 j and k), only poleward flow at the coast in the upper 300m was observed.

As indicated by the doming of the isotachs, the poleward undercurrent on the shelf break appeared to lie between the two equatorward surface flows. When these two surface currents were observed to be distinct and penetrating-to-depth (e.g. March), the poleward flow followed similarly i.e. was also distinct and large. The poleward undercurrent appeared to remain in this position nestled between the two surface flows over the whole year, except in October and November. Corresponding to the onshore movement of the surface currents as in June, the poleward current appeared to follow. In addition, as the basic shape of the surface currents changed, the poleward current followed, for example, in May the surface currents became shallower and broader together with the poleward current but at all times remained in contact with the shelf. In October and November the core of the surface currents were situated very close to the coast, possibly inhibiting poleward flow. Poleward flow remained over the slope and did not entrain to the surface in this case.

The bottom poleward flow at the coast appeared to be related to the surface currents in a manner as described above. This flow is small and confined to the coastline from December to April and moved at an average poleward speed of 1cm.s^{-1}. In months where the surface currents were distinct it appeared as its own distinguishable poleward flow but when the characteristics of the surface currents changed it did similarly in conjunction with the above flows. Intermittently the poleward flow over the shelf break extended over the shelf and the two poleward flows appeared to merge. As with the disappearance of poleward flow over the

shelf break in October and November, this poleward current was suppressed over the period but returned in December.

There did not appear to be seasonality to the structure of the alongshore current. Since wind stress varies seasonally, any effect it exerts on the nature of the equatorward flow is expected to have some degree of seasonality. On average, the seasonal effect of wind is not seen, but in summer to autumn (January to April) the two equatorward surface flows were more distinct and appeared to have more structure than the other months. Winter and spring, appeared to be more variable with the shape of the flow varying between months. Equatorward wind stress in summer could possibly effect equatorward flow substantially to maintain the structures seen in Figures 3.6 a -d.

The behaviour of the isotachs is considered further in Figures 4.8 to 4.10, where the results of moorings at four locations are displayed.

Figures 4.6 (a-l) show the standard deviation of alongshore current of the transect in the vertical, with the isolines spaced at 1cm.s^{-1} intervals. Maximum variability in alongshore current was observed to be at the surface and is consistent with the equatorward surface currents. This suggests that within each month, the current at those regions vary considerably both temporally and spatially. Standard deviation along the bottom remained smaller than the surface values but compared to the maximum current speeds of 5cm.s^{-1} and 1cm.s^{-1} are comparatively large (3cm.s^{-1}). Low values of variability over the slope suggest that the movement of water at the bottom was a relatively common, stable process. The gradients of the standard deviation isolines became progressively steeper from January through summer suggesting that there was a noticeable distinction in the opposing alongshore current flow. This occurred as the poleward current intensified in magnitude and spatial structure.

Significant doming of the variability isolines was apparent in October through December. Variability reached a maximum of 17cm.s^{-1} at the surface. There were apparent "cores" of variability i.e. at a certain region maximum variability occurs and decreases in a concentric spatial pattern around this central area. This

possibly indicates that the surface currents were highly variable during this period, with most of the variability occurring within the depths reached by the surface currents, although the surface currents may penetrate further into the water column at various periods during the month. This does not imply that there was an absence of the poleward undercurrent close to the coast during October and November but due to the large variability of the region, it was not apparent on average.

By studying the Hovmöller plot of the currents in the upper 50m of the water column for the transect, discussed next, the temporal behaviour of the surface currents may become more apparent.

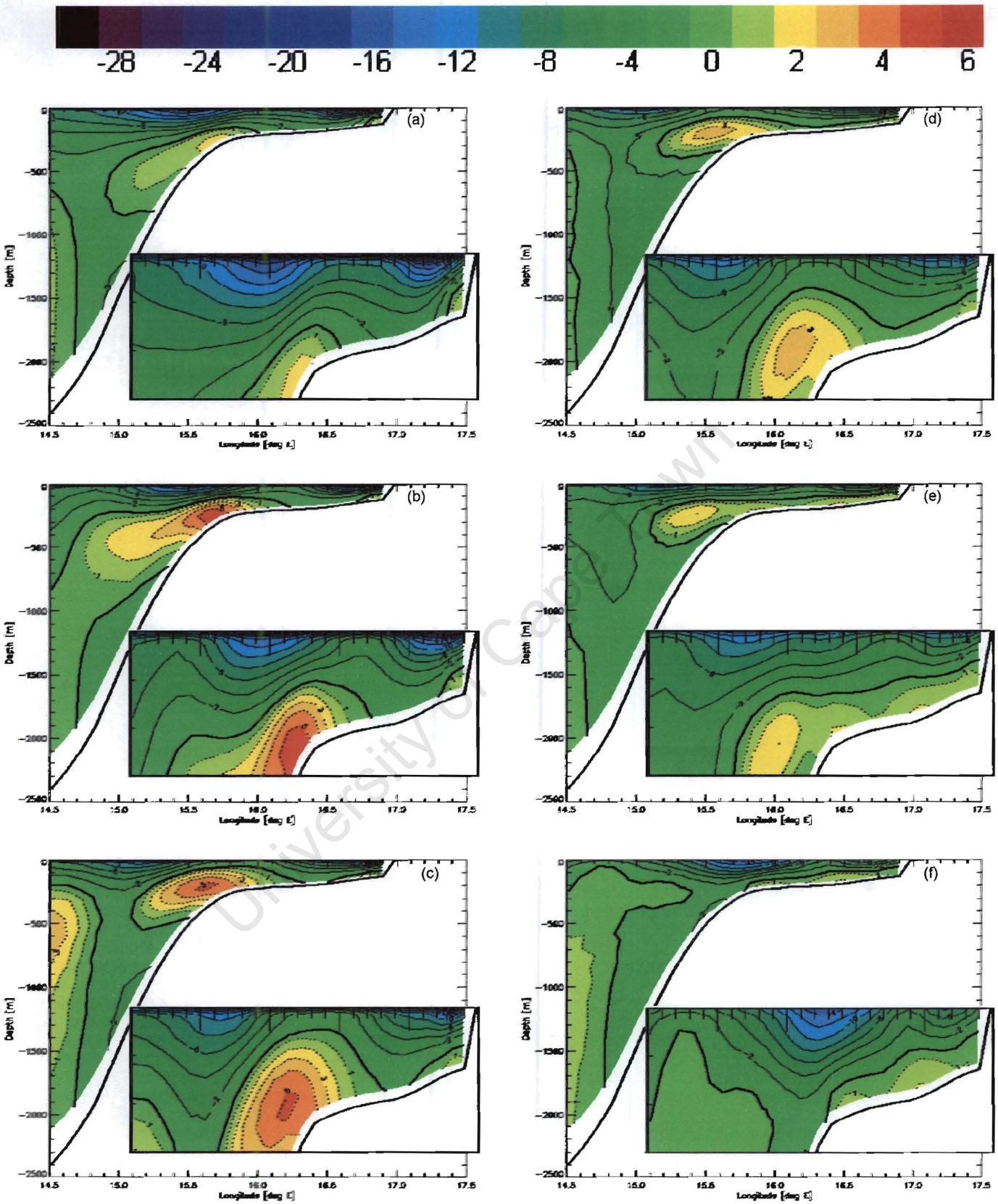

Figure 4.5 (a - f): Vertical section of the monthly climatology of alongshore current ($cm.s^{-1}$) for the transect (January – June).
Solid line = equatorward flow, dashed line = poleward flow. Bold line = O $cm.s^{-1}$ isotach.
Inset: Zoom of upper 300m of section.

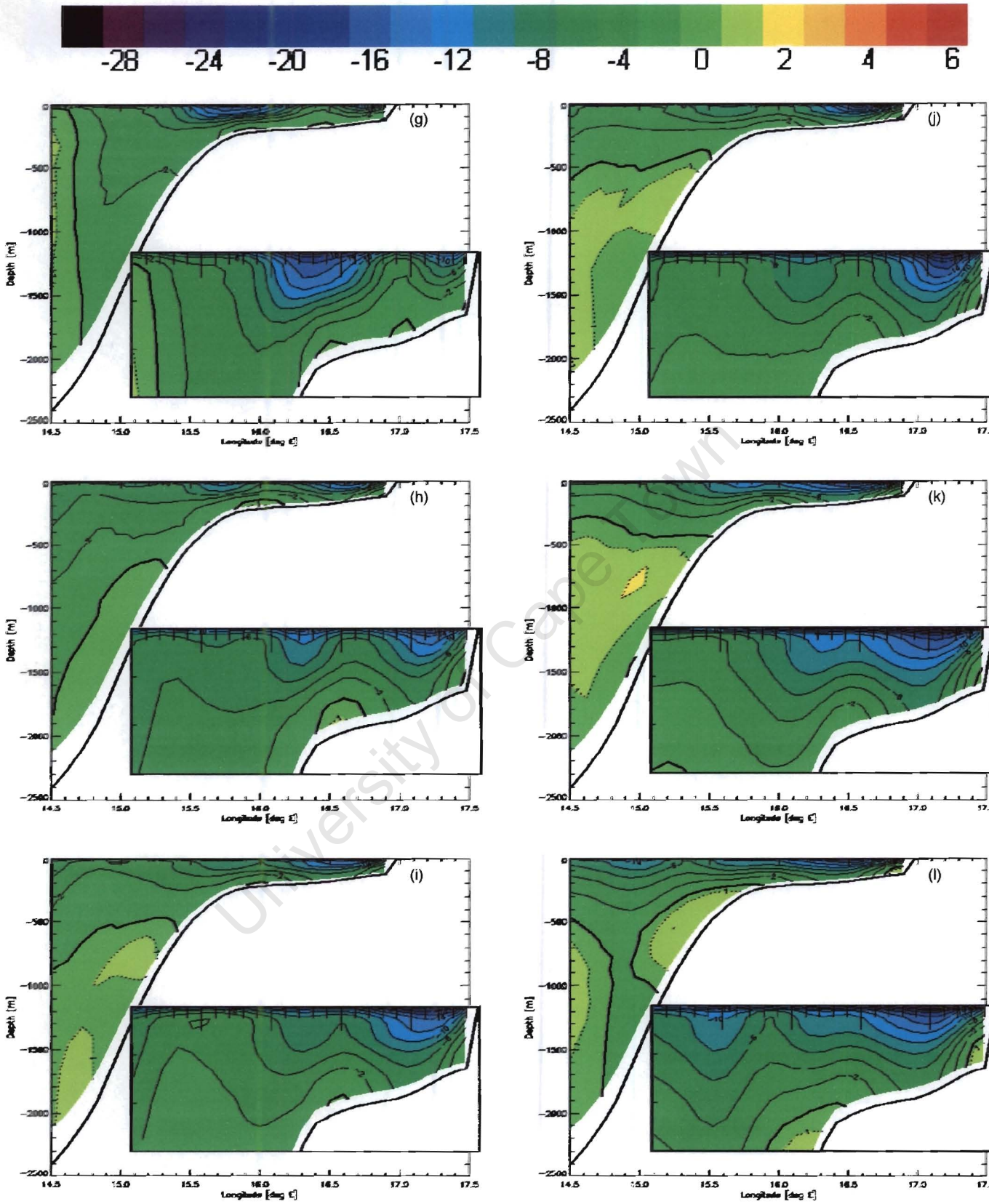

Figure 4.5 (g - l): Vertical section of the monthly climatology of alongshore current ($cm.s^{-1}$) for the transect (July – December).
Solid line = equatorward flow, dashed line = poleward flow. Bold line = O $cm.s^{-1}$ isotach.
Inset: Zoom of upper 300m of section.

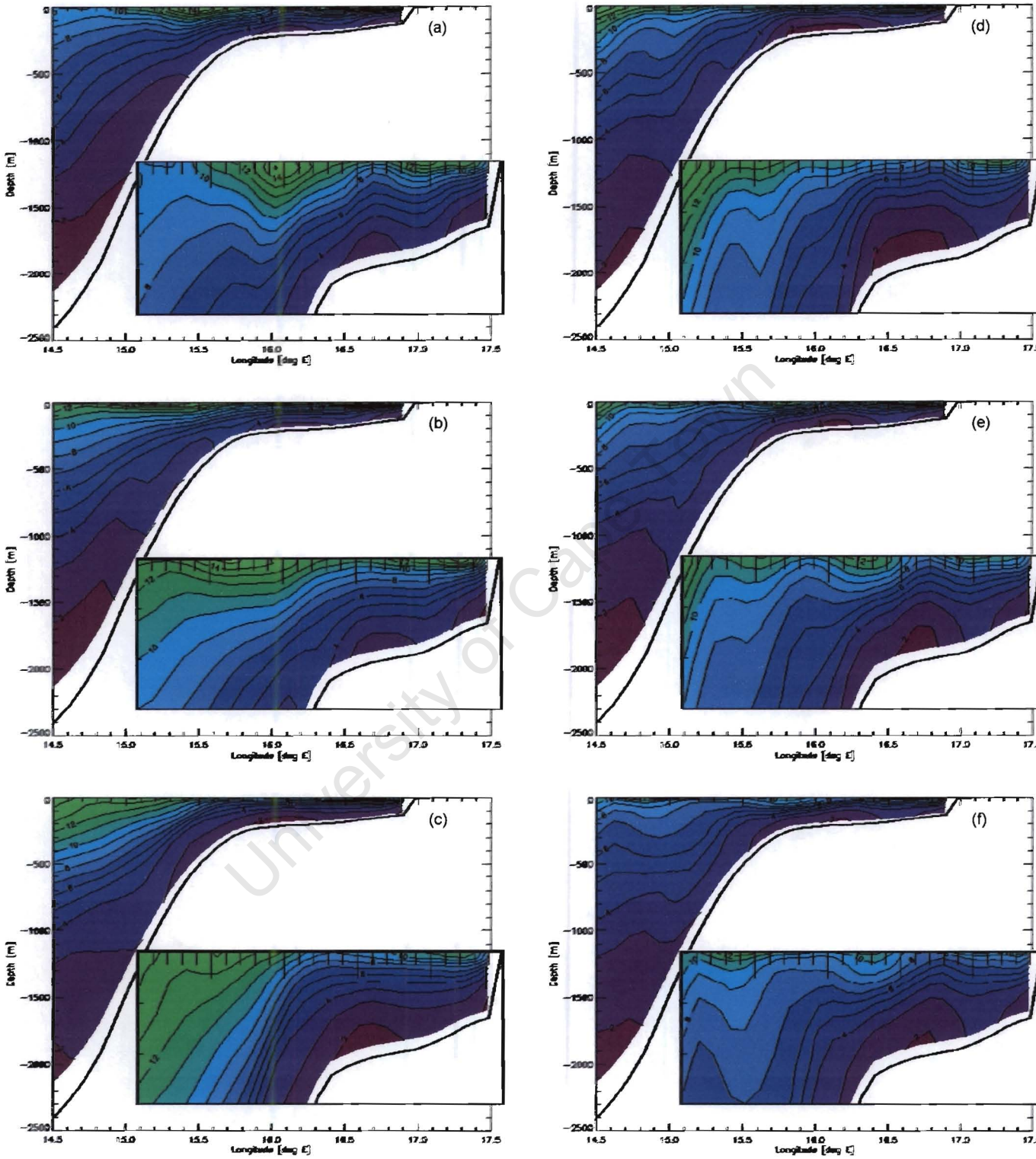

Figure 4.6 (a - f): Vertical section of the standard deviation of alongshore current ($cm.s^{-1}$) for the transect (January – June).
Inset: Zoom of upper 300m of section.

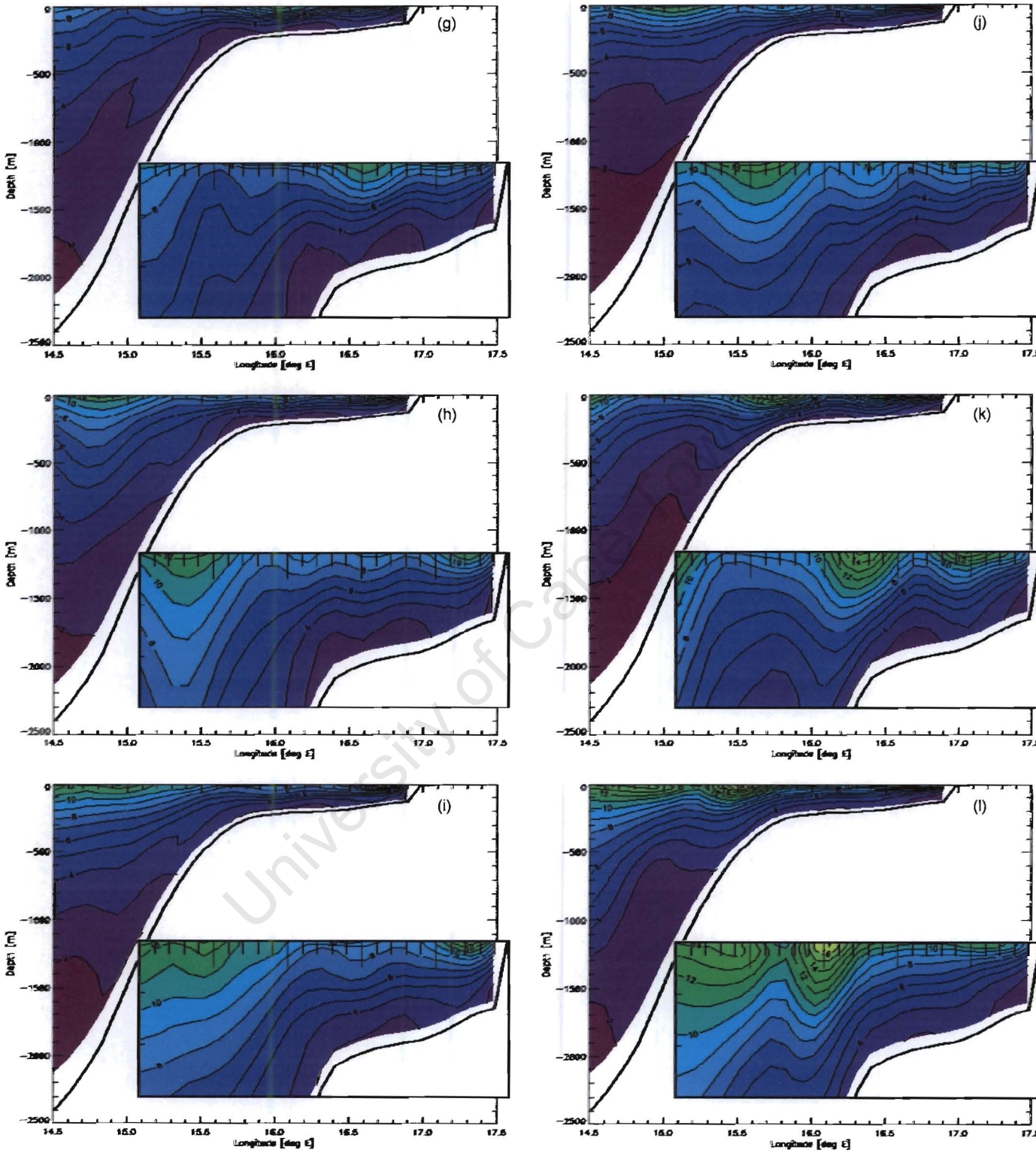

Figure 4.6 (g - l): Vertical section of the standard deviation of alongshore current ($cm.s^{-1}$) for the transect (July – December).
Inset: Zoom of upper 300m of section.

Hovmöller Plots of the Transect

The temporal characteristics of the upper 50m of the ocean along the transect for the year, is indicated by the use of the Hovmöller plot. As the data used for this plot is derived from the climatology it is indicative of the mean behaviour of the ocean surface over 10 years.

Temperatures close to the coast are of significant value as they are indicative of the presence of upwelling throughout the year. As shown in the temperature Hovmöller plot (Figure 4.7a), there was constantly cold water between 13 and 14°C on the coast. This water reached a constant offshore extent throughout most of the year except in June, when no existence of water below 15°C was observed. The 15°C isotherm displayed very little seasonal variation, remaining consistently between 16.8 and 16.9 °E, i.e. it varied by only 1° of longitude, roughly 110km. The 15°C isotherm reached its maximum offshore extent mid-August. In this region offshore, around the 15° isotherm, temperatures changed by 2°C within 3 to 4 degrees of longitude. Compared to the gradients of isotherms offshore, this region could be host to a front indicating the offshore extent of upwelled water - although this is considered a naïve approach to finding the frontal position. This "front" was observable in summer and transitional months (mid-October to April) when upwelling was expected and at its most intense. In months associated with decreased alongshore wind stress (May to September), the isotherms were less compressed, suggesting a break-down in upwelling over these months (upwelling did occur but was minimal).

As discussed earlier in the vertical section, the 16°C water did not originate at depth but was standard at the surface. In summer, temperatures offshore became warmer with distance away from the upwelling front, reaching a maximum of 20°C in January and February. Offshore to about 16.5°E, water reached 16°C. Between June and September, this 16°C water extended further offshore than this longitude, reaching a maximum 15.8°E in mid-August. Following the isotherms, the water offshore was observed to become cooler as summer progressed to

winter until the water offshore, along the transect west of the 16°C isotherm was a consistent 17°C between August and mid-October.

As seen in Figure 4.8a, temperature varies by between 0.4 and 0.8 °C for most of the year. Close to the coast east of 16.5°E, the region of highest temperature variability was found. As observed, the summer months January to March, displayed the maximum temperature variability, with temperatures varying by up to 1.2 °C offshore over the shelf and 1.6°C over the shelf break and shelf. This is consistent with varying wind stress and possible intense upwelling events causing large variations in temperatures offshore.

The cross-shore currents in the upper 50m (Figure 4.7b) yield the surface movement of the water in the Benguela Upwelling Region, the dashed line indicates that the cross-shore velocity direction of flow is onshore while the solid line indicates offshore flow. Water over the transect, for the year appeared to be relatively variable with mainly an offshore component with a periodic flow of water onshore centred at 16.4°E and 14.5°E. Close to the coast the flow was highly variable in direction varying from offshore to onshore with mean onshore flow extending to regions centred around 16.4°E from February to July. The water in this coastal region moved offshore with a speed of up to $4cm.s^{-1}$ in summer but in winter reached up to $8cm.s^{-1}$. Also observed in this region were consistent areas of non-motion, $0cm.s^{-1}$ isotachs, where offshore flow changed to onshore flow, suggesting that adjacent to the coast, the water moved offshore.

Between 16 and 16.5°E the cross-shore component was completely in the offshore direction. The region to the west of 15.5°E was more variable with the existence of onshore and offshore components. West of this region, there were periods with strong onshore flow (April, May and August) with speeds reaching $4cm.s^{-1}$, when compared to Figure 4.3 it was found that onshore flow penetrated to above 50m thus causing a mean that was onshore. In summer, two appearances of very strong offshore flow was found: in late January / early February centred around 15.5°E and mid-March centred around 15°E both reaching $16cm.s^{-1}$.

Standard deviation plot (Figure 4.8b) shows that the cross-shore current varied mostly by 8-10 $cm.s^{-1}$. In March through April variability west of 15°E was found to reach a maximum $16cm.s^{-1}$ coinciding with the large amount of onshore flow close to the surface.

As seen in the monthly, vertical section of alongshore current speed and standard deviation (Figures 3.5 and 3.6 respectively), current at the surface was mainly equatorward. The Hovmöller plot of alongshore current, Figure 4.7c showed that on average the transect in the upper 50m was consistent over time. Flow was consistently equatorward with mean speeds between $8\text{-}14cm.s^{-1}$, except in June and July where two regions display average poleward surface flow, this was possibly due to the poleward flowing water through most of the water column that had moved east and was enough to effect the last stations of the transect.

Flow at the coast, displayed a seasonality that was not obvious in the vertical sections. From September through February the surface flow was equatorward at speeds up to $20cm.s^{-1}$ compared to the period from April to July where speeds ranged from 8-14 $cm.s^{-1}$. The latter period corresponded to the high variability of the surface waters discussed earlier.

In the region, between 15.5 and 16°E the current intensity appeared to vary largely over the year. Here, the alongshore current was at its most intense in January, June and July (up to $16cm.s^{-1}$) but weaker for the rest of the year, except in March. In March the flow was predominantly poleward, this corresponds to Figure 4.5c where the poleward undercurrent reached surface waters thus influencing mean flow in this surface layer. Since standard deviation (Figure 4.8c) was not unusually high, this suggests that the poleward undercurrent is consistently at a spatial and intensity maximum through this time period.

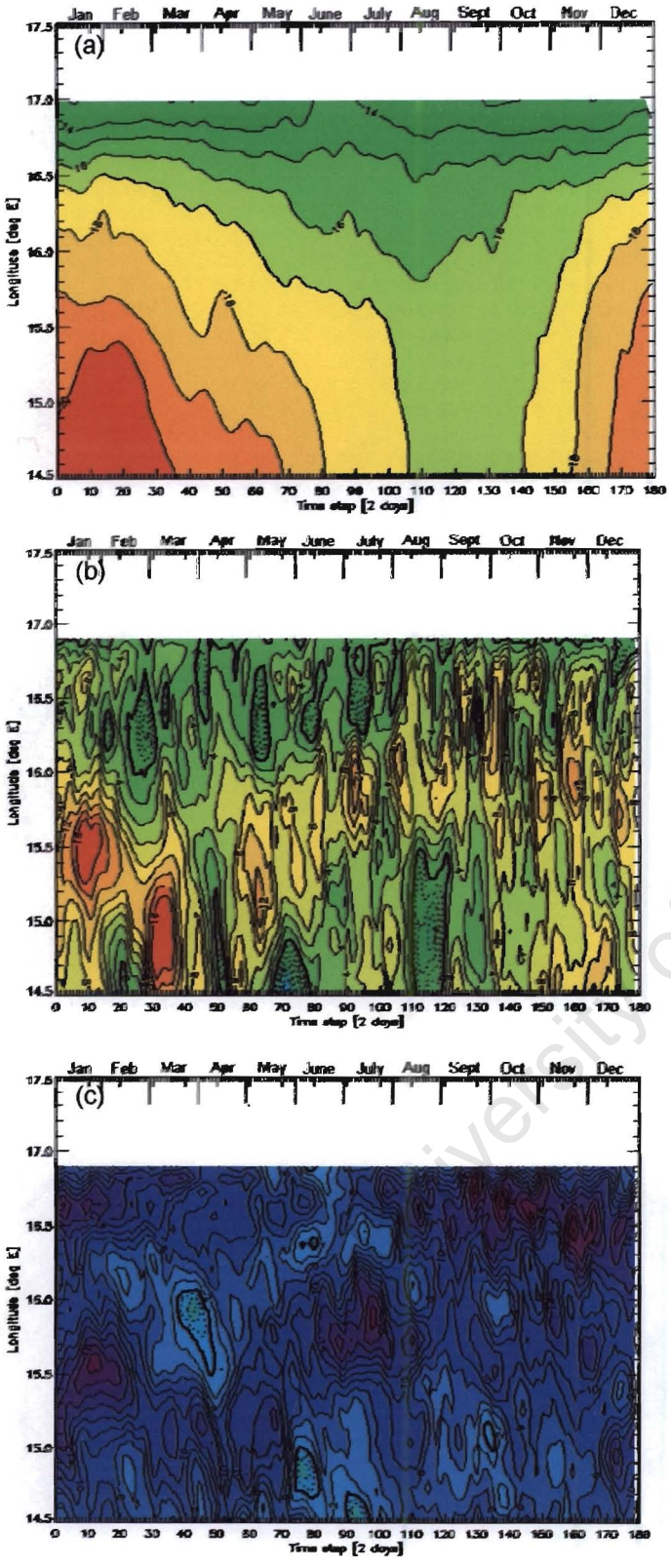

Figure 4.7: Hovmöller plot over the transect of
(a) Temperature (°C)
(b) Cross-shore current (cm.s^{-1})
(c) Alongshore current (cm.s^{-1}).
Solid line = equatorward/ offshore flow, dashed line = poleward/ onshore flow. Bold line = O cm.s^{-1} isotach.

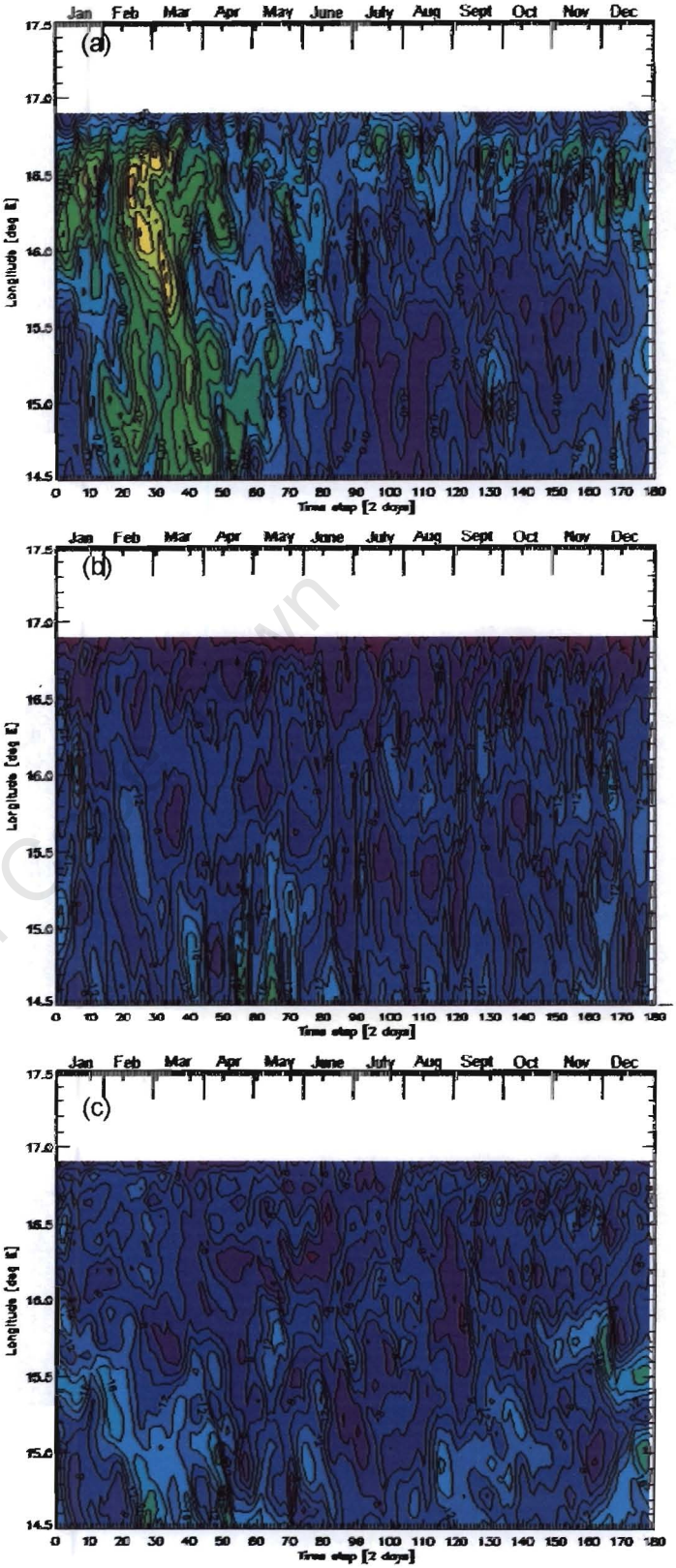

Figure 4.8: Hovmöller plot over the transect of standard deviation for:
(a) Temperature (°C)
(b) Cross-shore current (cm.s^{-1})
(c) Alongshore current (cm.s^{-1}).
Solid line = equatorward/ offshore flow, dashed line = poleward/ onshore flow. Bold line = O cm.s^{-1} isotach.

Moorings

The four moorings over specifically different regions reflect the movement of water as it moved onto the shelf. In this section when "flow" is referred to, it indicates spatial distribution enclosed by the isotachs and the magnitude of the current itself.

Mooring A

Mooring A at the coast revealed that mean surface temperature throughout the year (Figure 4.9) varied from 11 to 15°C. The water column appeared stable with warmer water overlying cooler waters. Surface waters in the upper 30m were generally 14°C but in summer the upper 20m reached a mean temperature of 15°C as observed in December. Cold water at 11°C was present at the bottom in summer and lay in a layer of 50m thickness from January to April. In May to mid-June the thickness of this layer decreased and eventually was not present in July and August. From September this layer increased in thickness as summer approached.

As observed by the 0 $cm.s^{-1}$ isotach in cross-shore current (Figure 4.9b), the water above 30m is observed to be predominantly offshore at the coast while below this, the flow tended to be onshore, reaching speeds of up to 2 $cm.s^{-1}$. In this surface layer at the coast, water tended to move offshore at speeds of up to 10 $cm.s^{-1}$ in summer. In winter, speeds decreased reaching up to 4 $cm.s^{-1}$ as observed in June and July.

Alongshore current data (Figure 4.9c) revealed that poleward flow was present at the coast in a bottom layer, varying in thickness from 5 to 90m over the period from November. In July and from mid-September to mid-October this feature was not present. If increased wind stress affected the alongshore flow, the intense, deep-penetrating sections of alongshore current could indicate this. The isotachs appeared to peak just once a month where alongshore flow decreased suggesting a coastal signal that is consistent over the years.

Mooring B

For Mooring B, found mid-shelf (Figure 4.10a), the temperature ranged from 11 to 19°C. As in the coastal mooring, Mooring A, the bottom layer of 11°C water decreased in thickness in August and September. At the surface the temperature became much warmer than at the coast, probably due to the cold upwelled waters being confined to lower depths and not having reached the surface. From May to September only 15°C water was found at the surface while from October surface temperatures started warming due to seasonal effects.

A large, thick layer of onshore flow was present at the bottom of this mooring (Figure 4.10b). Overlying this layer, offshore flow occurred and was observed to have maximum speeds in November. It appeared that the more intense the surface offshore flow, the weaker and shallower the onshore bottom layer. This was possibly due to the interactions at the surface, the more intense the wind forcing the larger the reaction of the ocean surface, i.e. stronger winds will cause divergence of the surface ocean to greater depths, suppressing onshore flow lower down the water column. Thus with weaker winds, there will be less offshore surface flow and greater (in speed and distribution) onshore flow at depth.

Mooring B showed very little poleward flow along the bottom (Figure 4.10c), most of the flow was observed to be equatorward with maximum speeds observed in November. As indicated by the isotachs, flow at this mooring was maximum in summer. Between the recurrent surface current features, a succession of depressed isotachs were observed in some months and lasting about 2 weeks, suggesting periods of fast and deep equatorward flow. The many events were separated by very steep gradients implying that surface flow at the mid-shelf was highly variable throughout the year.

Mooring C

At the shelf break, Mooring C (Figure 4.11a), the temperature structure was similar to that mid-shelf with summer associated with warmer surface water overlying cold water at the bottom. The bathymetry over which the mooring lies is deeper than Moorings A and B and thus records a minimum temperature of 10°C.

Over the shelf break from November to June, the cross-shore current plot (Figure 4.11b) showed that onshore flow was apparent at the bottom of the water column. Initially, this onshore flow was confined to the bathymetry but was observed to move at mid-depths in the water column from April to June and then again in the period from July to September in 3 events lasting roughly 10 days each. Onshore flow for cross-shore current was observed to be maximum in February. In months such as September and October, onshore flow was not found at the shelf break. In January offshore flow was observed to be fast (about 18cm.s^{-1}) and deep (extending below 160m) and onshore flow minimal (between 40 and 90 m thick).

At Mooring C, alongshore current (Figure 4.11c) was predominantly equatorward throughout the water column but was disrupted by an extensive layer of poleward flow from December to May (with maximum thickness in March / April). This poleward flow grew in thickness from January to March until it occupied the entire water column in April. At its most intense the poleward flow reached 7cm.s^{-1}. In comparison, the equatorward current reached speeds of up to 22cm.s^{-1}. From June to July maximum equatorward flow was observed with speeds of 10cm.s^{-1} at depths of 120m. Sharp gradients in this plot suggest that this region over the shelf break is highly variable, where characteristics of magnitude and direction change over a short period of time.

Mooring D

Mooring D (Figure 4.12a), located along the continental slope and coinciding with the region found in Blanke *et al.* (2002), showed similar surface seasonal patterns down to depths of 150m. The alongshore current vertical sections (Figures 4.5 c & d) showed that poleward flow was maximum during March and April. In these months the mooring displayed a divergence between the 11°C and 12°C isotherms, with each isotherm radiating in opposing directions, emphasising the presence of the poleward flow.

In the cross-shore current time plot (Figure 4.12b), it was observed that the maximum offshore flow occurred in summer. Also observed were regions of onshore flow, water from various depths moving onto the slope. Through most of the year, onshore-flowing water occurs at the bottom flowing along the continental slope.

Over the slope between July and January (Figure 4.12c), a poleward flow in contact with the slope was observed. In the months proceeding January, this poleward flow detached and shoaled over time. Between mid-June and mid-July there was a disappearance of the poleward flow. The poleward current then resumed the pattern from a thickening layer in contact with the shelf to the intense current structures seen from February to mid-June. Equatorward current speed was maximum at the surface and reached approximately 15cm.s^{-1}. Overlying the intense poleward flow, an expansion of isotachs over 200m (usually associated with the upper 20m) was observed. The latter half of the year displayed a consistent sluggish equatorward flow (around 2 to 6cm.s^{-1}) above 500m and overlying the poleward undercurrent, except for the highly variable surface 20m.

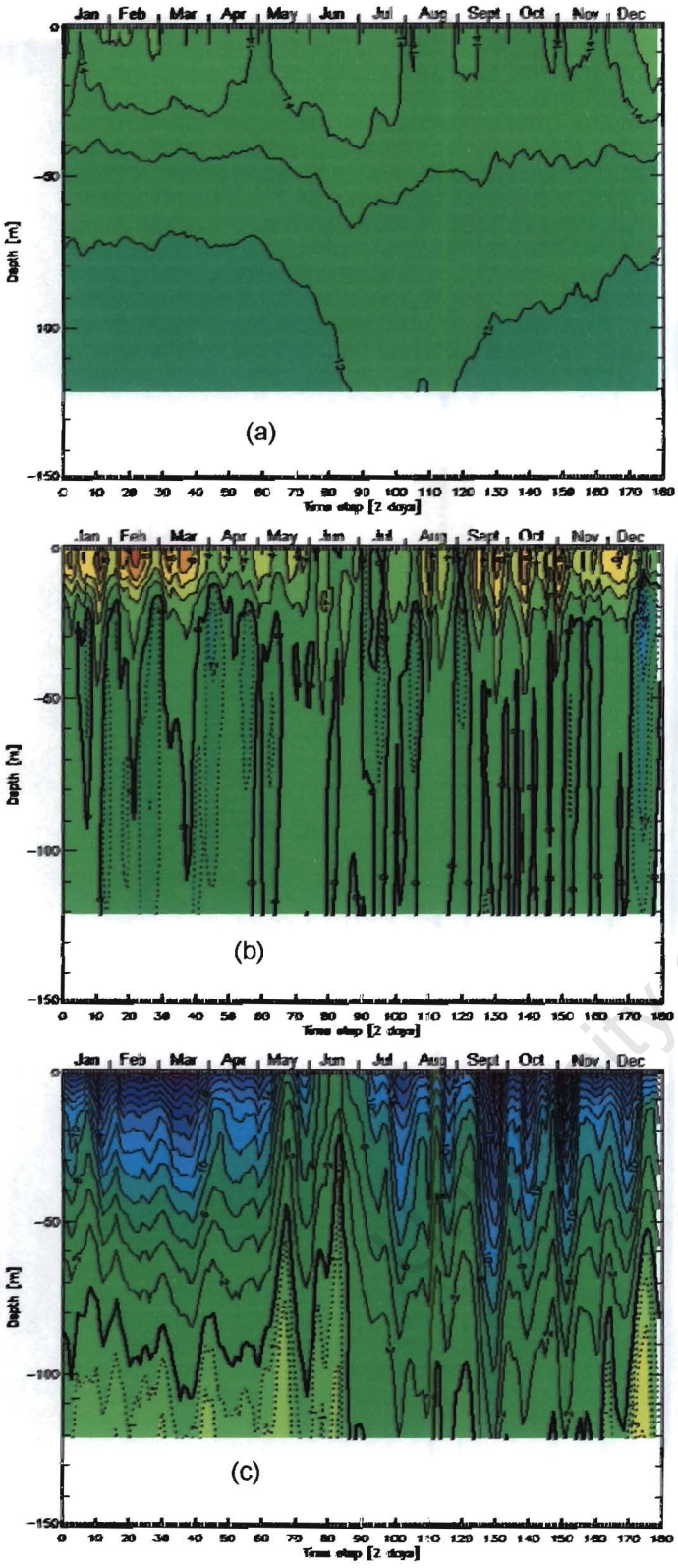

Figure 4.9: Climatological time series with depth for Mooring A of:
(a) temperature (°C)
(b) cross-shore current (cm. s^{-1})
(c) alongshore current (cm. s^{-1}).
Solid line = equatorward/ offshore flow,
dashed line = poleward/ onshore flow.
Bold line = O cm.s^{-1} isotach.

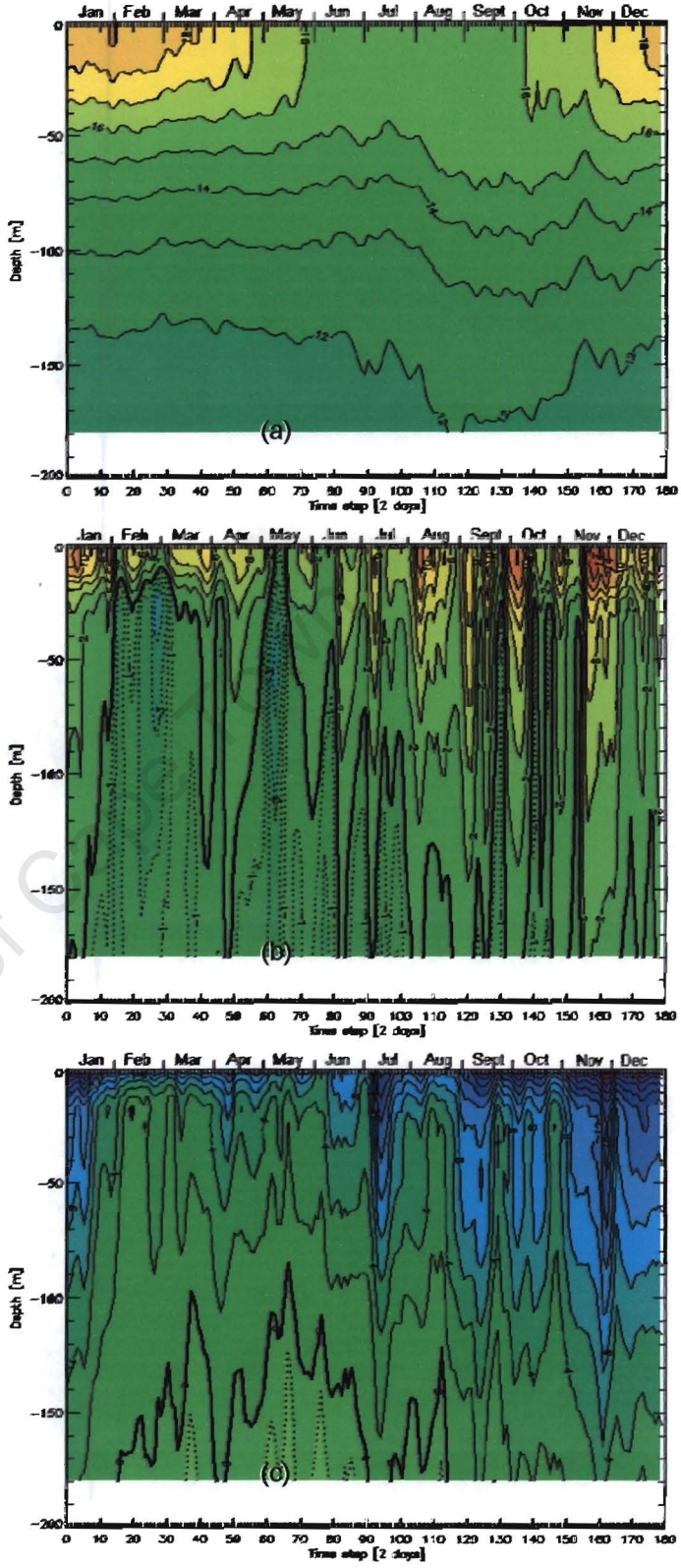

Figure 4.10: Climatological time series with depth for Mooring B of:
(a) temperature(°C)
(b) cross-shore current (cm. s^{-1})
(c) alongshore current (cm. s^{-1}).
Solid line = equatorward/ offshore flow,
dashed line = poleward/ onshore flow.
Bold line = O cm.s^{-1} isotach.

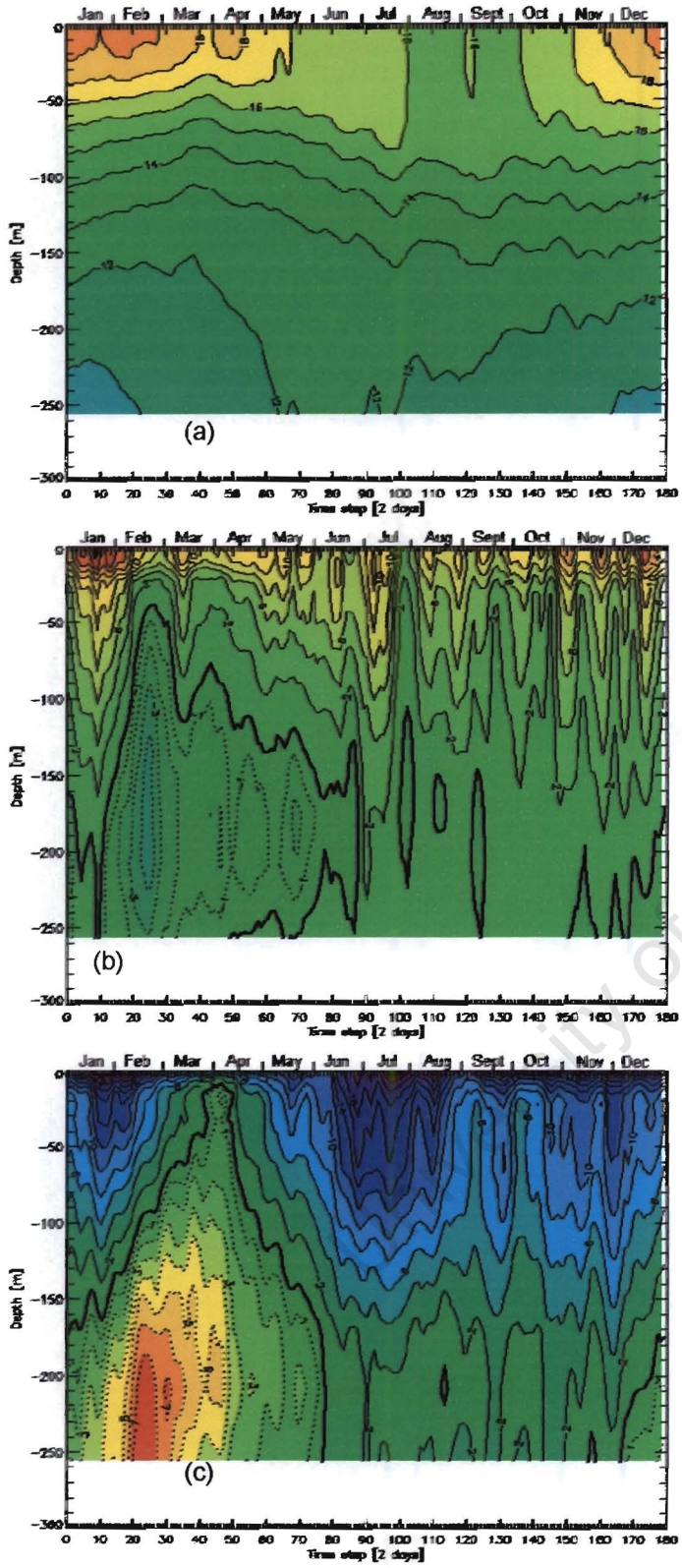

Figure 4.11: Climatological time series with depth for Mooring C of:

(a) temperature (°C)
(b) cross-shore current (cm. s^{-1})
(c) longshore current (cm. s^{-1}).

Solid line = equatorward/ offshore flow,
dashed line = poleward/ onshore flow.
Bold line = O cm.s^{-1} isotach.

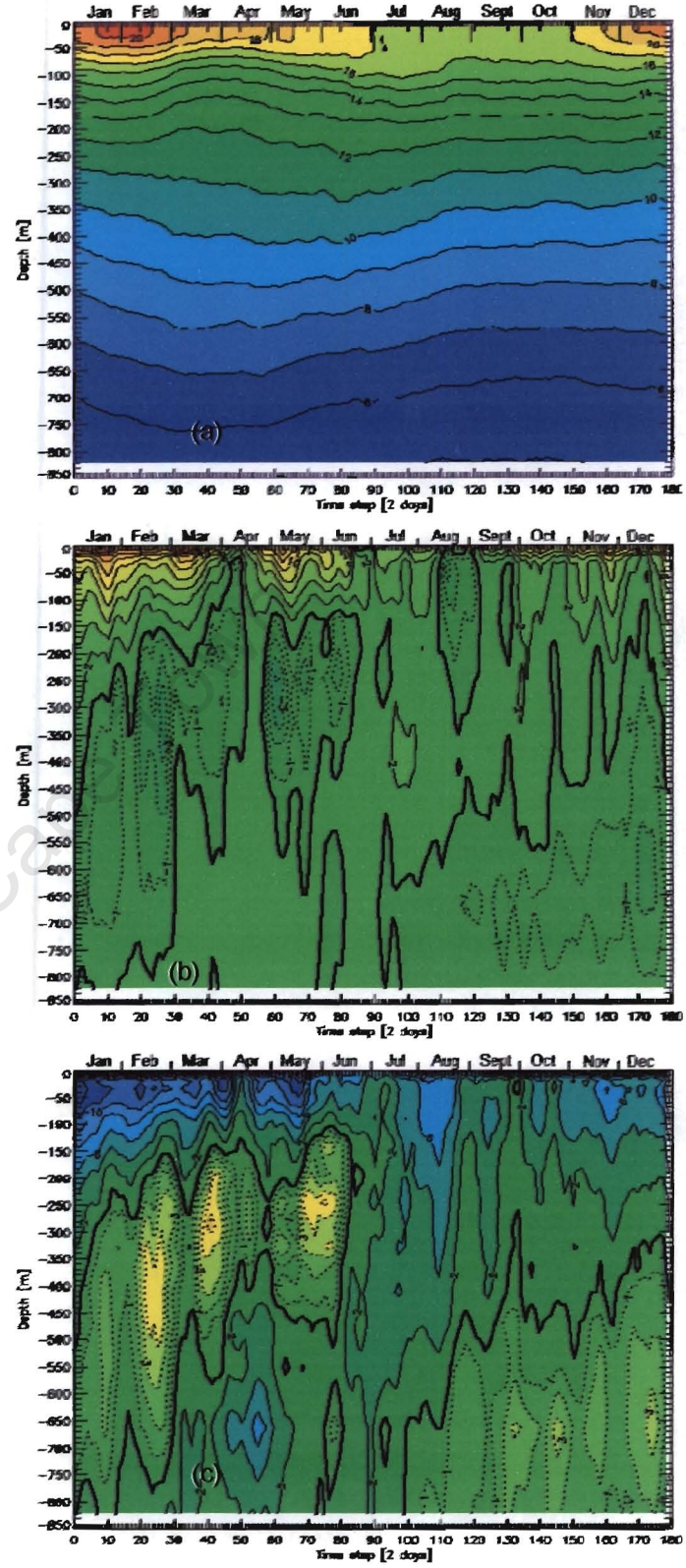

Figure 4.12: Climatological time series with depth for Moorin D of:

(a) temperature (°C)
(b) cross-shore current (cm. s^{-1})
(c) longshore current (cm. s^{-1}).

Solid line = equatorward/ offshore flow,
dashed line = poleward/ onshore flow.
Bold line = O cm.s^{-1} isotach.

Isotherms

Figures 4.13 and 4.14 show the depth of particular isotherms throughout the year, for two of the moorings, Mooring D (over the slope) and Mooring B (mid-shelf). In Figure 4.14, Mooring D displayed isotherms between 8°C and 16°C, as these encompass the primary water temperature range expected when investigating upwelling. Fewer isotherms were plotted in 4.13, the mid-shelf mooring, as not all cool upwelled water reached the shelf. Missing data for the 16°C isotherm in Figure 4.13 occurred where the 16°C isotherm did not extend onto the shelf over Mooring B, this is also seen in Figure 4.10a where 16°C water was missing from the surface waters from June through September.

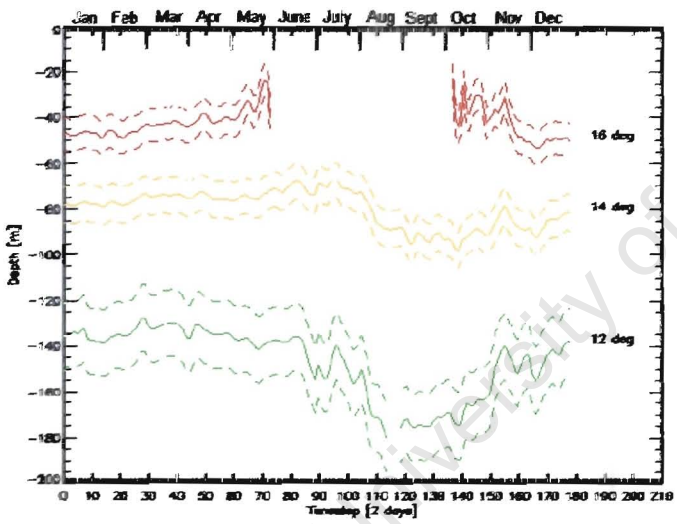

Figure 4.13: Depth of isotherms (metres) over the mid-Shelf at Mooring B.
Dashed lines = standard deviation.

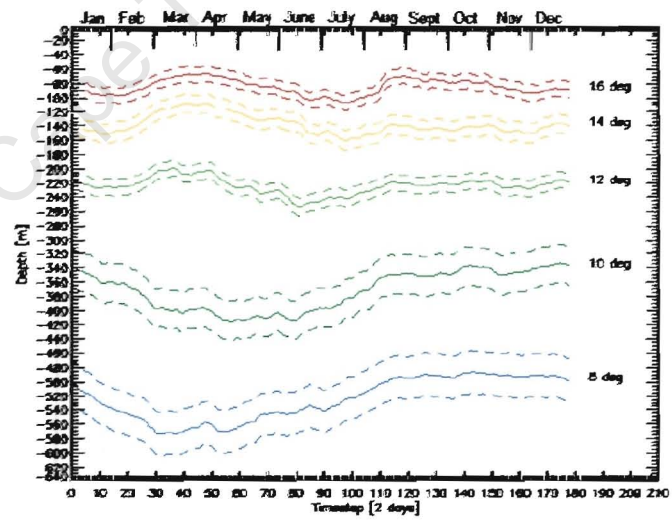

Figure 4.14: Depth of isotherms (metres) over the continental slope at Mooring D.
Dashed lines = standard deviation.

It was observed that 16°C water was not present over the shelf during winter (Figure 4.13). Also observed was a depression in the 12 and 14°C isotherms from July to October. This is probably due to decreased upwelling in winter, therefore less cool waters from below flow onto the shelf and shoal to the upper water column.

Over the slope, all isotherms between 8 and 16°C were present throughout the year. The 12, 14 and 16°C isotherms displayed a small standard deviation (of approximately 20, 30 and 20m respectively) as compared to the 8 and 10°C isotherms which were more variable (standard deviation of approximately 70m each). These isotherms were positively displaced in summer and negatively displaced in winter. There appeared to be two separate patterns in the isotherms over the year: the 12 to 16°C isotherms above 250m and those below. The two patterns were in opposition from mid-December until May for the 10°C isotherm and March for the 8°C. The negative displacement was indicative of the presence of the poleward undercurrent above it. For the rest of the year, the 8 and 10°C isotherms were positively displaced suggesting that the waters upwelled along the slope at this point. The 12 to 16°C isotherms from January to mid-June displayed a positive displacement suggesting upwelling. Thereafter isotherms remained at a fairly constant level. From August to November, all isotherms over the slope appeared to be parallel. This suggests a decline in the poleward undercurrent and upwelling.

5. Discussion

In this section, the hydrography in combination with the spatial and temporal characteristics are discussed to obtain a general picture of the nature of the chosen transect as well as the processes involved.

Monthly Climatological Behaviour of Isolines

The temperature sections appeared to reflect the classical view of upwelling. Surface temperatures were cooler over the slope in winter and warmer in summer. Ekman transport (offshore surface flow) was more intense in summer with water upwelling from below onto the shelf. Over mid-slope, onshore flow existed throughout the year. From December, the first indication of water moving from the slope onto the shelf was observed; as summer progressed, this upwelling water proceeded to reach the shelf and eventually the coastline in February. In May, the upwelling over the shelf diminished and receded over the shelf leaving remnants of this water on the shelf close to the coastline. This was probably due to the relaxation of winds during winter causing the topography to have an enhanced effect.

The upwelling season for this region was observed to be from December to March with maximum upwelling occurring in February and maximum speeds in January. Throughout the year there was an onshore flow of water confined to the coast irrespective of the occurrence of upwelling.

Equatorward surface currents in the upper 10m were intense throughout the year but less so in winter. The poleward current was found to occur from December and May and reached a maximum speed of 5cm.s^{-1}. From May only remnants of the poleward undercurrent remained. These remnants, located on the shelf, then diminished and were not present in October and November. When surface

equatorward currents were maximum, the equatorward flow (with its two cores) was also maximum. For the most part of the year there was a presence of subsurface poleward flow at the coastline which, like the poleward undercurrent, reflected the behaviour of the surface flow. Poleward flow appeared to occur where the change in topography is the greatest, i.e. at the shelf break and the bottom of the continental rise.

Surface flow could possibly be disrupted by the poleward undercurrent over the shelf break causing the equatorward flow to reflect two maxima or cores. However, contrary to this, this could be the branching of the Benguela Current mentioned in Stramma and Peterson (1989). By comparison of the cross-shore and alongshore currents, poleward flow was observed to always be accompanied by onshore flow, with strong poleward flow corresponding to strong onshore flow. The poleward flow could be moved up onto the shelf and into the hollow of the dome caused by the branching Benguela Current.

The poleward undercurrent at the shelf break did not appear to inhibit upwelling onto the shelf. Rather, upwelling coincided with poleward flow displaying a direct relationship between their intensity and spatial distribution, furthermore both only appeared in conjunction with each other.

Variability was observed to increase over areas with large changes in topography such as the shelf break and at the continental rise.

Surface Behaviour of Transect

Cold water of 13 to 15°C was present at the coast in the upper 50m throughout the year. Further offshore, waters displayed seasonal characteristics with waters being warmer in summer and cooler in winter. Highest temperature variability occurred at the coast and over the whole transect during summer with a maximum in February. The 15°C with its uniform position was simplistically considered the offshore extent of upwelled waters.

The cross-shore currents in the upper 50m appeared to be comparatively variable with mainly offshore flow at the coast to 16°E, periodic onshore flow was observed occurring at locations centred at 16.4°E and 14.5°E. Offshore flow was observed to be maximum in summer. Maximum variability occurred when upwelling was strong and expansive. Alongshore surface flow was predominantly equatorward with poleward flow occurring where the poleward flow was spatially maximum. Equatorward flow at the coast was observed to be maximum in summer with winter flow being, on average, slower and more variable.

Flow of water from the slope

As seen by the very sharp gradients observed in current behaviour the currents are highly variable with time for each of the chosen regions.

Mid-slope extending to 820m the whole range of possible isotherms were observed up to 20°C, temperatures were obviously warmer in summer at the surface. Divergence of isotherms indicating the presence of the poleward undercurrent was observed. Progression of the poleward undercurrent and upwelling were observed starting mid-year and moving up the shelf. Offshore and equatorward flow were observed to be spatially largest when the opposing flows are shallow.

At the shelf-break, temperature was more variable but similar surface warming was observed. Offshore surface flow was maximum in summer while equatorward flow appeared similar throughout the year but decreased in summer/autumn when poleward flow was maximum. Onshore and poleward flow at the bottom occurred mainly in summer.

Mid-shelf closer to the coast, temperature though still showing seasonality at the surface, was generally cooler. A substantial part of the water column reflected onshore flow, attached to the bottom, throughout most of the year but was maximum from February to May. Some poleward flow was observed at the bottom at this location. The core of equatorward flow was confined to a thin layer at the surface above this poleward structure, while at times when the poleward flow did not appear the equatorward current was strong and deep.

At the coast, temperatures were consistently cool. Currents were highly variable but directed mostly offshore in the upper 20m while at the bottom the water was mostly onshore. To a depth of 90m the current was in an equatorward direction, below this poleward flow attached to the bottom occurred.

6. Concluding Remarks

Due to the time limitation allocated to this thesis, an investigation of the wind data was considered beyond the scope of the project. The data set used comprised of a full 2-day time series of temperature, cross-shore and alongshore currents for 10 years. Combining the above data, there is the potential to obtain much knowledge on the response of the southern Benguela to wind forcing as well as the many processes and structures involved. Using the full resolution of temperature anomalies together with the wind data, anomalous occurrences of wind conditions and associated processes could also be investigated. Since model data are a complement to *in situ* data, comparative studies could be performed to confirm the viability of this method

REFERENCES

Blanke, B., Roy, C., Speich, S., McWilliams, J. & Nelson, G. (2002). Linking wind and interannual upwelling variability in a regional model of the southern Benguela [Electronic Version]. Geophysical Research Letters, 29(24). Retrieved February 27, 2003 from http://www.agu.org.

Boyd, A.J. (1987). The Oceanography of the Namibian Shelf. PhD Thesis, University of Cape Town, 190pp.

Cole, J. & Villacastin, C. (2000). Sea Surface temperature variability in the northern Benguela upwelling system, and implications for fisheries research. International Journal of Remote Sensing, 21(8), 1597-1617.

Da Silva, A.M., Young, C.C., & Levitus, S. (1994). Atlas of surface marine data 1994, volume 1, algorithms and procedures. NOAA Atlas NESDIS 6, U.S. Department of Commerce, NOAA, NESDIS, USA.

Fennel, W. (1999). Theory of the Benguela Upwelling System. Journal of Physical Oceanography, 29, 177–190.

Garzoli, S.L., & Gordon, A.L. (1996). Origins and variability of the Benguela Current. Journal of Geophysical Research, 101(C1), 897-906.

Garzoli, S.L., Gordon, A.L., Kamenkovich, V., Pillsbury, D., & Duncombe-Rae, C. (1996). Variability and sources of the southeastern Atlantic circulation. Journal of Marine Research, 54(6), 1039-1071.

Gordon, A.L., Weiss, R.F., Smethie Jr., W.F., & Warner, M.J. (1992). Thermocline and intermediate water communication between the South Atlantic and Indian Oceans. Journal of Geophysical Research, 97(C5), 7223-7240.

Hagen, E., Feistel, R., Agenbag, J.J., & Ohde, T. (2001). Seasonal and interannual changes in Intense Benguela Upwelling (1982-1999). Oceanologica Acta, 24(6), 557-568.

Haidvogel, D.B., & Beckmann, A. (1998). Numerical Models of the Coastal Ocean. In K.H. Brink & A.R. Robinson (Eds.), The Sea, Vol. 10. The global coastal ocean: processes and methods (pp. 123 - 234). New York: John Wiley & Sons, Inc.

Haney, R. L. (1991). On the pressure force over steep topography in sigma coordinate Ocean models. Journal of Physical Oceanography, 21, 610-619.

Hart, T.J., & Currie, R.I. (1960). The Benguela Current. Discovery Report, 31, 123-297.

Holden, C.J. (1987). Observations of low-frequency currents and continental shelf waves along the west coast of South Africa. In A.I.L. Payne, J.A. Gulland & K.H. Brink (Eds.), The Benguela and comparable frontal systems, (pp. 197-208). South African Journal of Marine Science, 5.

Jury, M.R. (1988). Case studies of the response and spatial distribution of wind-driven upwelling off the coast of Africa: 19-34° south. Continental Shelf Research, 8(11), 1257-1271.

Jury, M.R., & Courtney, S. (1995). Climatic determinants of Benguela SST variability. Continental Shelf Research, 15(11/12), 1339-1354.

Kantha, L.H., & Clayson, C.A. (2000). Numerical models of oceans and oceanic processes. San Diego: Academic Press.

Lima, I.D., Garcia, C.A.E., & Möller, O.O. (1996). Ocean surface processes on the southern Brazilian shelf: characterization and seasonal variability. Continental Shelf Research, 16(10), 1307-1317.

Merino, M. (1997). Upwelling on the Yucatan Shelf: hydrographic evidence. Journal of Marine Systems, 13, 101-121.

Nelson, G. (1992). Equatorward wind and atmospheric pressure spectra as metrics for primary productivity in the Benguela Upwelling System. In A.I.L. Payne, K.H. Brink, K.H. Mann & R. Hilborne (Eds.), Benguela Trophic Functioning, (pp. 19-28). South African Journal of Marine Science, 12.

Nelson, G., Boyd, A.J., Agenbag, J.J., & Duncombe Rae, C.M. (1998). An upwelling filament north-west of cape Town, South Africa. In S.C. Pillar, C.L. Moloney, A.I.L. Payne & F.A. Shillington (Eds.), Benguela dynamics: impacts of variability on shelf-sea environments and their living resources, (pp. 75-88). South African Journal of Marine Science, 19.

Nelson, G. & Hutchings, L. (1983). The Benguela Upwelling Area. Progress in Oceanography, 12, 333-356.

Noble, M.A., & Ramp, S.R. (2000). Subtidal currents over the central California slope: evidence for offshore veering of the undercurrent and for direct, wind-driven slope currents. Deep-Sea Research II, 47, 871-906

Olson, D.B., Fine, R.A., & Gordon, A.L. (1992). Convective modification of water masses in the Agulhas. Deep-Sea Research, Suppl. 1, S163-S181.

Penduff, T. (1998). Étude de la dynamique de l'Atlantique Nord-Est à l'aide d'un modèle numérique régionale. PhD thesis, Université de Bretagne Occidentale, Brest.

Penven, P. (2000). A numerical study of the Southern Benguela circulation with an application to fish recruitment. PhD thesis, Université de Bretagne Occidentale, Brest.

Penven, P., Roy, C., Brundrit, G.B., Colin de Verdiere, A., Freon, P., Johnson, A.S., Lutjeharms, J.R.E. & Shillington, F.A. (2001). A regional hydrodynamic model of upwelling in the Southern Benguela. South African Journal of Science, (97), 472-475.

Reid, J.L. (1989). On the total geostrophic circulation of the South Atlantic Ocean: flow patterns, tracers and transports. Progress in Oceanography, 33, 1-92.

Shannon, L.V., Boyd, A.J., Brundrit, G.B, & Taunton-Clark, J. (1986). On the existence of El Niño-type phenomenon in the Benguela system. Journal of Marine Research, 44(3), 495-520.

Shannon, L.V. & Nelson, G. (1996). The Benguela: Large Scale Features & Processes & System Variability. In G. Wefer, W.H. Berger, G. Siedler & D.J. Webb (Eds.), The South Atlantic: Present & Past Circulation (pp 163 – 210). Berlin Heidelberg: Springer-Verlag.

Shillington, F.A. (1998). The Benguela Upwelling System off Southwestern Africa. In A.R. Robinson & K.H. Brink (Eds.), The Sea, Vol. 11. The global coastal ocean: regional studies and syntheses (pp 583 – 603). New York: John Wiley & Sons, Inc.

Skogen, M.D. (1999). A biophysical model applied to the Benguela System. South African Journal of Marine Science, 21, 235-249.

Stander, G.H. (1967). The Benguela Current off South West Africa. South Africa. Department of Commerce and Industries. Division of Sea Fisheries. Fisheries Bulletin, 4, 1-7.

Stramma, L. and Peterson, R.G. (1989). Geostrophic Transport in the Benguela Current Region. Journal of Physical Oceanography, 19, 1440- 1448.

Sverdrup, H.U., Johnson, M.W., & Fleming, R.H. (1942). The oceans, their physics, chemistry, and general biology. New York: Prentice-Hall, Inc.

Tomczak, M. (1996). Atlantic Ocean. Retrieved March 4, 2003, from http://www.met.ed.ac.uk/calmet/conferences/calmet01/cd/tomczak/oceanography/regoc/text/14circ.html.

Tyson, P.D. (1986). Climate change and variability in Southern Africa. Cape Town: Oxford University Press.

Van Foreest, D., Shillington, F.A. & Legeckis, T. (1984). Large scale, stationary, frontal features in the Benguela Current system. Continental Shelf Research, 3(4), 465-474.

ACKNOWLEDGEMENTS

I would like to express my sincere appreciation to my supervisors Dr. Claude Roy and Assoc. Prof. Frank Shillington for the assistance in planning and executing this project as well as the constant support and open door.

To the Oceanography Department, thank you for the support. I am indebted to Prof. Geoff Brundrit, for his help and support throughout my degree. I would also like to thank Dr. Christian Mullon and Carolina Parada for assistance with the model. I am grateful to my fellow (in)mates in the dungeon for the help and especially in getting through coursework. Special thanks to Tarron Lamont for assisting me with her knowledge and moral support. To Nazeera Hargey and Jenny Veitch thanks for listening to my whining and for lunches upstairs. To Helen Stewart, your presence in the department has made working on campus a pleasure.

The financial support of my sponsors, Thales Geosolutions (South Africa) (PTY) Ltd., is gratefully acknowledged and I would like to thank Prof. Geoff Brundrit and Bruce Spolander for facilitating the scholarship.

Thanks to Pevash Naidoo (a.k.a. Pinky) and Roary (the only stuffed tiger to be mentioned in a thesis) for all the support and offering sound advice whilst working with me in the labs until the ridiculous hours of the morning. I would like to express my gratitude to the following people who have provided moral support: Keethal, Umoyo, Nawahl, Cath, Nadine, Chris and Genevieve.

Finally, all credit must go to my parents for their guidance.